Sensors & Diagnostics

PERSPECTIVE

View Article Online
View Journal | View Issue

Cite this: *Sens. Diagn.*, 2024, **3**, 987

Modified synthetic peptides: from therapeutics to chemosensors

Conor Wynne [ab] and Robert B. P. Elmes *[ab]

Modified synthetic peptides have emerged as an exciting avenue for enhancing therapeutic efficacy and expanding the scope of applications in various disease contexts. Indeed, the inherent tunability of synthetic peptides has facilitated the creation of highly selective and responsive sensors capable of detecting specific analytes with precision. More recently, their unique structural diversity and chemical versatility has been elegantly adapted for use in supramolecular sensing platforms. This Perspective article highlights the synergistic interplay between modified synthetic peptides, therapeutic applications, and the sensing technologies that underscore the interdisciplinary nature of contemporary chemistry.

Received 16th January 2024,
Accepted 3rd April 2024

DOI: 10.1039/d4sd00022f

rsc.li/sensors

[a] *Department of Chemistry, Maynooth University, National University of Ireland, Maynooth, Co. Kildare, Ireland. E-mail: robert.elmes@mu.ie*
[b] *Synthesis and Solid-State Pharmaceutical Centre (SSPC), Bernal Institute, University of Limerick, Castletroy, Co. Limerick, Ireland*

Conor Wynne

Conor Wynne achieved his BSc (Hons) in Pharmaceutical & Biomedical Chemistry at Maynooth University (MU) in 2019. He is now pursuing his PhD under the supervision of Dr Robert Elmes within the Chemistry Department at MU, where he utilises Solid-Phase Peptide techniques to generate responsive synthetic peptide conjugates, with applications in various disease contexts. His research interests are around the use of modified synthetic peptides as fluorescent/luminescent sensors and novel peptidomimetics.

Robert B. P. Elmes

Rob graduated with a B.A. Mod. in Medicinal Chemistry from Trinity College Dublin in 2007 before he was awarded an IRCSET Embark Scholarship to undertake his PhD under the supervision of Prof. Thorri Gunnlaugsson at TCD. After a short postdoctoral tenure at the Trinity Biomedical Sciences Institute in Dublin, Rob moved to The University of Sydney under the guidance of Prof. Kate Jolliffe where he was involved in the development of new platforms for the recognition, sensing and transport of biologically relevant anions. In late 2014, Rob returned to Ireland taking up a lecturing position at Maynooth University where he is currently Associate Professor and Associate Dean of Research for the Faculty of Science and Engineering. He has enjoyed periods as an invited researcher at Universite d'Orleans, in France in the Centre for Molecular Biophysics and at The Scripps Research Institute in La Jolla, California and is a funded investigator at the SSPC, Ireland's Pharmaceutical Research Centre and the Kathleen Lonsdale Institute for Human Health Research at Maynooth University. Rob's research interests lie in the fields of Supramolecular Chemistry and Chemical Biology where the group is trying to use supramolecular chemistry to develop new drug delivery vehicles, diagnostic tools, and novel approaches to treating microbial infections.

Introduction

Historical notes

Peptides are physiologically active compounds made up of short chains of amino acid (AA) monomers connected by amide bonds (peptide bonds). The beginning of peptide chemistry has long been attributed to the year 1901, when chemists Emil Fischer, and Ernest Fourneau published the first ever "synthetic peptide" – a dipeptide called glycyl-glycine (Gly-Gly).[1] One of the most significant scientific successes in peptide drug discovery was the development of insulin, a peptide containing 51 amino acids. It was discovered in 1921 by Frederick Banting and further refined by Frederick and Charles Best.[2,3] Peptide chemistry received little attention for the next 30 years, until the medicinal use of peptides really kicked off after World War 2. Following this, oxytocin was synthesized by du Vigneaud in 1953, a major achievement for peptide chemistry and a synthetic milestone.[4] However, these methods required a huge amount of time and synthetic effort for even the most trivial of peptides. It wasn't until Bruce Merrifield revolutionised peptide chemistry in 1963 with Solid-Phase Peptide Synthesis (SPPS).[5] This technology pioneered the way for quick, easy, and efficient preparation of peptides, and was the basis for his 1984 Nobel Prize in Chemistry. SPPS substantially accelerated progress across the chemical and medicinal sciences. Furthermore, peptide's inherent specificity and excellent efficacy have made them attractive building blocks for the design of novel therapeutics.[6]

Clinical use of peptides

Peptides are frequently involved in human physiology, acting as hormones,[7] neurotransmitters,[8] growth factors,[9] or ion channel ligands.[10] Moreover, peptides tend to act as intrinsic signalling molecules for many of these physiological functions, opening up the possibility for peptide-therapeutic mediation that closely resembles the natural process.[11] Indeed, utilising peptide-based therapeutics has been commercially proven to help treat many diseases/disorders such as, type 2 diabetes, multiple sclerosis, acromegaly and osteoporosis – with the likes of Eli Lilly (Trulicity™), Novo Nordisk (Victoza™) and Novartis (Sandostatin™) dominating this space (Fig. 1).[12]

In recent years, over 60 peptide drugs have been approved by the US-FDA, Europe, and Japan: over 150 are in active clinical development, and an additional 260 have been tested in human clinical trials.[10,13] This translates to a global peptide therapeutics market currently valued at $37.8bn (US dollars), with projected growth of 9.6% (CAGR) to $91.25bn by 2031 (Fig. 2).[14] Over 21 peptide therapeutics are currently being utilised to treat COVID-19, including 15 synthetic peptides in development against SARS-Cov-2 infection-related respiratory disorders.[15] Peptide therapeutics are also being examined as a COVID-19 treatment option. As a result, significant industry participants reported a rise in revenue during the COVID-19 epidemic.[14] Through the many lockdowns and long working-from-home periods, much of the population experienced more sedentary lifestyles. Coupled with the corresponding bad habits and unhealthy diets, a surge in chronic disease prevalence and incidence may be on the horizon. To this end, the worldwide peptide therapeutics market is likely to be driven by an increase in metabolic disorders forecast for the coming years.[16]

Peptides interact with cell-surface receptors and cascade intracellular reactions with high affinity and specificity, similar to large biologics such as proteins and antibodies.[17] However, peptide-therapeutics provoke less of an immune response and typically have reduced production costs.[18,19] Small-molecule drugs also benefit from low production costs and tend to have good oral bioavailability and membrane permeability.[20] On the other hand, the clinical use of small-molecule therapeutics can be restricted due to their low specificity compared to peptide drugs. Peptide-based therapeutics usually have two inherent shortcomings: their ability to penetrate the cell-membrane(s) to reach intracellular targets, and *in vivo* stability – as their amide bonds can be hydrolysed by domestic enzymes.[21] These inherent benefits and drawbacks of peptide therapeutics provide both challenges in peptide drug development, as well as opportunities for peptide design and drug discovery. Peptides remain a distinct family of pharmaceutical compounds that are molecularly positioned somewhere

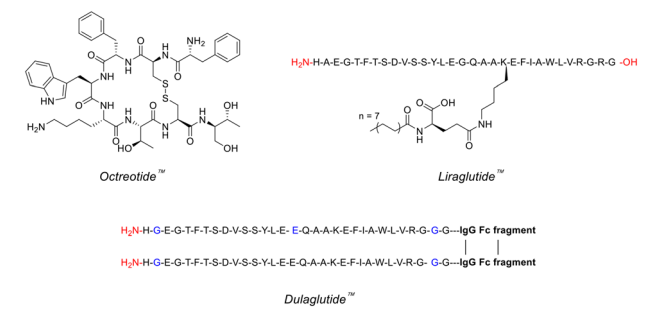

Fig. 1 Chemical structures of famous peptide therapeutics (single-letter abbreviations used for amino acids to ensure clarity).

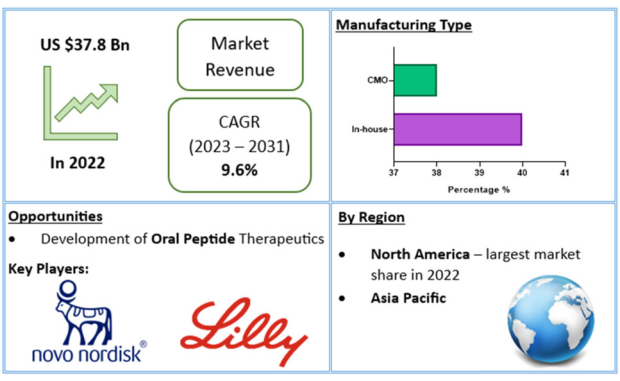

Fig. 2 Global peptide therapeutics market value and financial forecasts.[14]

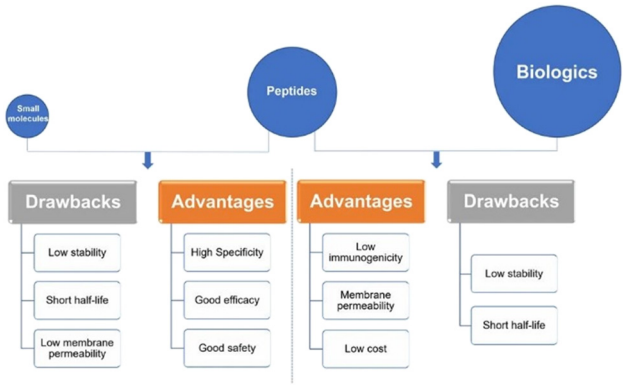

Fig. 3 Peptides *versus* small molecules and biologics. Comparison of advantages and drawbacks between peptides and small molecules or biologics (reprinted from ref. 22 with permission from Springer Nature, copyright 2022).[22]

between small molecules and proteins (Fig. 3), while being biochemically and therapeutically distinct from both.[22]

Peptides as building blocks in supramolecular chemistry

Peptides can also play a crucial role as building blocks in supramolecular chemistry – a field that focuses on the study and design of molecular assemblies beyond individual molecules. The importance of peptides in supramolecular chemistry lies within their unique structural and functional properties, which make them versatile and valuable components for creating complex and functional materials.

The potential sequence variability provided by the 20 natural amino acids presents a significant opportunity for investigating optimal building blocks conducive to specific self-assembling characteristics, leveraging their diverse attributes in terms of charge, hydrophobicity, and polarity.[23] Incorporation of non-natural amino acids into peptide sequences has also been employed to augment the diversity of self-assembling peptides and enhance the complexity of the resulting self-assembled structures.[24] In addition to the primary structures determined by the amino acid sequence, peptides also exhibit distinct secondary structures. These inherent secondary structures can function as foundational units for elevated levels of self-assembly.[25] Consequently, peptides prove highly adept for hierarchical assembly, representing a potent yet intricate method for producing functional materials. The establishment of secondary (and more advanced peptide structures) is notably influenced by hydrogen bonding, predominantly originating from polar amide-, amino-, and carboxyl-groups present in both the backbone and the side chains of peptides.

Achieving effective peptide self-assembly has been exemplified through the utilisation of amphiphilic peptides, dendritic peptides, polypeptides, cyclic peptides, and aromatic di-peptides (Fig. 4).[26,27]

Frequently, the peptide sequences are crafted by employing biologically-inspired strategies, resulting in self-

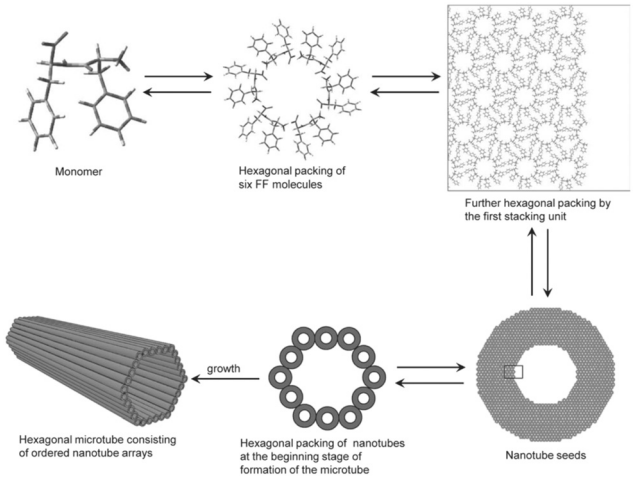

Fig. 4 Schematic illustration of the formation of hexagonal peptide microtubes *via* L-Phe-L-Phe molecules (reprinted from ref. 28 with permission from John Wiley and Sons, copyright 2011).[28]

assembled materials with structures and properties closely resembling those found in nature. Peptide-based supramolecular materials can offer distinct advantages in many biomedical applications, including; tissue-engineering, drug delivery, antibacterial treatments, immunotherapy, and imaging.[29]

However, before we explore the applications of modified synthetic peptides, we must understand the chemical alterations that are available to amino acids. With that said, the next section will delve into the unique molecular interactions and synthetic versatility that peptides offer, allowing for the precise design and engineering of supramolecular architectures.

Chemical modification of peptides

Since Merrifield introduced us to SPPS back in 1963, research in the peptide space has grown remarkably. Although the classical methods of SPPS provided a vital boost for peptide synthesis, it was limited by the dramatic decrease in purity as the number of coupling steps increased.[30] Building on the success of the Boc and Fmoc protecting groups,[31] innovative amino acid protecting groups and new methodologies were incorporated to produce high quality peptide products with superb yields. One early-stage method was fragment condensation *via* prior thiol capture, but this technique suffered from racemisation and other reaction complications.[32] An improvement on this coupling reaction was achieved by Kent & co-workers by the chemoselective reaction of unprotected peptides, they coined this – native chemical ligation (NCL).[33] Other ligation methods include (but not limited to) expressed protein ligation (EPL),[34] the Staudinger ligation,[35] and "click" or "switch" peptide ligation.[36]

The biological activity of peptide therapeutics is closely related to their chemical structure. Sometimes the peptide

structure may need to be synthetically modified to achieve an optimal secondary structure for improved biological activity, while retaining stability, selectivity and solubility of the peptide product.[37] Peptide natural products – often isolated from secondary metabolites produced by plants and microorganisms – have gained the appreciation of many research groups and institutions, due to their fascinating biological activity.[38] Most proteins consist of the 20 natural amino acid residues together with some post-translational modifications (phosphorylation or disulfide bridging), however the peptide-containing secondary metabolites frequently incorporate an assortment of unorthodox amino acids.[39–41] For this reason, the introduction and/or manipulation of side-chain(s) within a peptide sequence presents a dynamic alternative to traditional peptide chemistry, with the possibility of generating many different analogues from one peptide precursor.[42]

Introduction of peptidomimetic-elements

The classification of peptidomimetics has been cultivated alongside the progress of synthetic peptides in recent years. The classification that will be used throughout this section is based on the modern taxonomy introduced by Grossmann.[43] His categorisation denotes four distinct classes of peptidomimetics – A, B, C and D – depending on their resemblance to the natural substrate.[44] Class A peptidomimetics closely resemble the parent peptide, utilising very few modified amino acids to stabilise the bio-active conformation, with modifications being restricted to the peptide backbone or sidechains. Next is class B peptidomimetics, featuring derivatives of class A mimetics with small-molecule insertions, uncanonical amino acids, and considerable backbone modifications. This class is home to peptoids and foldamers, where the backbones are extensively modified, but the side-chain functionalities are retained in the same order as the parent peptide.[45] Class C mimetics are more small-molecule in stature, containing an uncanonical framework that almost completely replaces the peptide backbone. The orientation of key residues is retained, and the bio-active conformation remains intact. However, the central scaffold bears little resemblance to that of the native peptide. The final category of peptidomimetics – class D – are a far-cry from the natural peptide. Class D molecules can emulate the mode-of-action of the natural peptide without a remotely similar backbone or side-chain functionalities.

Modification of peptide structures has been a growing area of research in recent years, with side-chain manipulations and backbone modifications being the two popular methods.

Side-chain modification. One method to achieve side-chain modification of peptides is to replace the canonical amino acids (AAs) with its structural analogue during peptide synthesis, this allows the peptide chemist a degree of synthetic flexibility to probe for increased binding affinity and selectivity.[46,47] Non-natural amino acids tend to induce protease resistance, such as derivatives of arginine – homoarginine, lysine, citrulline, ornithine, and *N*-isopropylornithine.[48]

Some side-chains are more difficult to modify than others, take valine and alanine for example – aliphatic side-chains without an obvious functional group present (Fig. 5) – there are relatively few techniques for derivatisation. However, recent breakthroughs in the direct functionalisation of C–H bonds have generated novel technologies for targeted modifications.[49] Of these recent breakthroughs, a notable example by Yu & group demonstrate the Pd-catalysed C–H arylation of N-terminal alanine residues.[50] The largest sequence that the group managed to modify using this technique was a tetra-peptide, nonetheless this preliminary study illuminates the (mostly) untapped potential of post-assembly C(sp^3)–H derivatisation as an exciting tool for the modification of aliphatic side-chains.

Like the aliphatic residues, the polar non-ionisable side-chains (primary amides) of glutamine and asparagine remain troublesome targets for derivatisation. Popp and Ball however, employed a molecular recognition strategy which facilitated the selective modification of the Gln and Asn side-chains using dirhodium metallo-peptides.[51] Reactions pursuing the modification of methionine however, are much

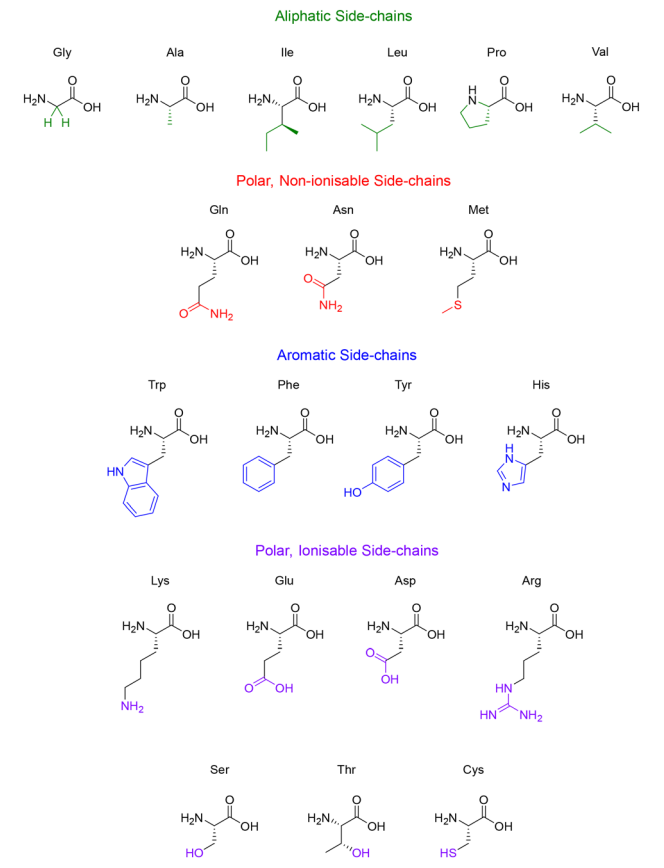

Fig. 5 The 20 natural amino acids categorised by their side-chain functionality.

more common. Methionine possesses a relatively high oxidation potential, and the reversible oxidation of the thioether is a well-described reaction pathway.[52] Interestingly, it is the only natural amino acid residue that can be alkylated under acidic conditions.[53]

Amino acid residues with aromatic side-chains tend to have a much larger pool of analogues to choose from, such as unnatural heterocycles,[54] and derivatives that include β-methyl groups for added conformational rigidity.[55] Aromatic side-chains can be further categorised into ionisable (tyrosine & histidine), and non-ionisable (phenylalanine & tryptophan). Barbas introduced us to a powerful new aqueous ene-type reaction that permits click-like Tyr coupling,[56] and has paved the way for the functionalisation of diverse handles, including PEG chains and multi-functional linkers.[57] Although the side-chain of tryptophan is regarded as non-ionisable, there still exists some potential for synthetic modification, as highlighted by the many specific reaction pathways available to the indole moiety. Indeed, these modifications are currently dominated by C–H functionalisation at the indole C-2 position.[58,59] This C–H functionalisation strategy has been used to facilitate alkynylation and arylation of the indole side-chain. However, similar approaches for the C–H functionalisation of the side-chain(s) for His and Phe remain underexplored. This represents an exciting challenge for researchers to develop novel methodologies to produce synthetically modified His and Phe residues.

Unsurprisingly, the amino acid residues with polar ionisable side-chains have been well-studied, with cysteine taking the top spot as the most documented residue within bioconjugation literature.[60] There are many properties of cysteine that make it a convenient target for side-chain modification, like its inherently low pK_a (~8.3) and the considerable nucleophilicity of the thiol group. Although the cysteine–maleimide conjugation has been a popular method of thiol modification,[61,62] the use of transition metals has gained recent recognition with the likes of Buchwald and Pentelute describing a Pd(II)-mediated arylation of Cys under mild conditions.[63] The theory described in this section serves to highlight the potential of side-chain modifications to introduce new functionalities or substituents into a given peptide natural product.

Backbone modification. The ADMET properties of peptides are intrinsically restricted, with many peptide therapeutics suffering from minimal absorption, poor distribution from the plasma, predominant renal excretion, a metabolic life-time that is critically limited to proteolytic cleavage, and therefore, may have toxicological implications.[46] Consequently, a key motive for backbone modification is to enhance the proteolytic stability of the peptide. Backbone modification often includes techniques like, insertion of methyl-AA,[64] incorporation of β-AAs,[65] peptoids,[66] and substituting L-AAs for D-AAs (Fig. 6).[67]

The introduction of these structurally diverse amino acids into the peptide sequence – even more so at the site of proteolysis – can be an effective method for increasing the plasma half-life of peptide therapeutics. An interesting example is selepressin – an analogue of vasopressin, containing the backbone modification [Phe$^{(2)}$, Ile$^{(3)}$, Hgn$^{(4)}$, Orn(iPr)$^{(8)}$] – which was being developed by Ferring Pharmaceuticals for the treatment of vasodilatory hypotension in septic shock.[68] Selepressin seen early clinical success, displaying comparable selectivity coupled with an enhanced plasma half-life. However, the phase 2b/3 clinical trial was terminated in February 2018 for futility, as the administration of selepressin, compared with placebo, did not result in any statistically significant improvement.[69] Perhaps further research is required to decide if selepressin will play a potential role in other patient-related conditions due to septic shock.

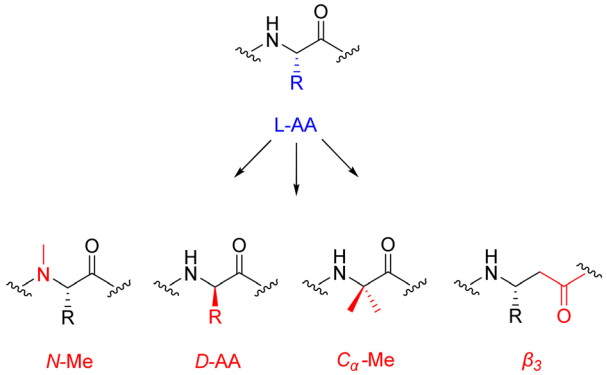

Fig. 6 Chemical structures of popular peptide backbone modifications.

Significant work regarding backbone modifications was pioneered by Seebach *et al.* who introduced side-chains into small peptides *via* enolate chemistry.[70] One of the groups most impressive applications of this technique is the site-selective alkylation of cyclosporin A,[71] where they demonstrate that the deprotonation of amide N–H bonds shields adjacent amino acids from deprotonation and prevents epimerisation. This process allowed the compound to undergo nucleophilic substitution with electrophiles to produce the modified cyclosporins in satisfactory yields (~90%) with a diastereomeric selectivity ratio of 5 : 1 (Re/Si, D/L).

As peptide chemists, the use of transition metals has allowed us access to previously unheard-of bioconjugate transformations, this is particularly true in the ever-expanding area of peptide backbone modification.[72,73] A recent example was inspired by known non-ribosomal peptide synthetase (NRPS) pathways, where researchers describe an iron-catalysed oxidative derivatisation.[74] This approach was utilised to generate 21 non-natural amino acids from 4 canonical residues while preserving the innate chirality. While this particular use of transition metals is scarce, the opportunities they present for peptide backbone modification, and protein structure/function will surely inspire innovation for novel peptide conjugates. The next

section will discuss a few of the main techniques used for the medicinal chemistry optimisation of peptides.

Macrocyclisation

Cyclisation is an essential strategy for the medicinal chemistry optimisation of peptide leads during drug discovery.[75,76] Cyclisation is an excellent method for improving the proteolytic stability of a target peptide. This allows medicinal chemists to take advantage of the high selectivity, increased potency, and low toxicity that are intrinsic to peptides, to progress them as potential biotherapeutic agents. An early example on the use of peptide-cyclisation during drug design was a cyclic analogue of somatostatin (Veber–Hirschmann peptide).[77] This newly cyclised peptide constrained the sequence into a bioactive conformation while also improving its proteolytic stability, resulting in a peptide-product with increased duration of action and oral bioavailability (Fig. 7). From this discovery, structural studies on other natural peptides were conducted to probe the use of cyclisation to explore novel bioactive conformations.[78]

As can be the case for many novel design scaffolds created by synthetic chemists, Nature did it first. Or at least provided the necessary inspiration to facilitate the discovery. The advantages imparted by cyclisation have been exploited by nature with the many cyclic peptides found in fungi, bacteria, plants, and animals.[79] One study by Craik *et al.* documented the effects of peptide-cyclisation on the structural-activity of sunflower trypsin inhibitor-1 (SFTI-1). This cyclic peptide is comprised of one cross-linking disulfide bond and is the smallest, most potent known inhibitor of trypsin.[80] The group observed that cyclisation was essential to its enzymatic stability and inhibitory activity (Fig. 8).[81] Many natural peptides like SFTI-1 possess exceptional chemical, thermal, and proteolytic stability, which can be (at least partially) attributed to their cyclic backbones. This section will examine the growing interest in macrocyclic peptides, and the various methods for synthesising cyclic peptides.

Synthetic considerations for cyclisation. In general, there are 4 main routes to facilitate peptide cyclisation: head-to-tail (N-terminus to C-terminus), head-to-side chain, side chain-to-tail, and side chain-to-side chain cyclisation (Fig. 9).

During the synthesis of cyclic peptides, the final ring-closing reaction can often be a lactonisation (cyclic carboxylic ester),[82] lactamisation (cyclic amide),[83] or produce disulfide-

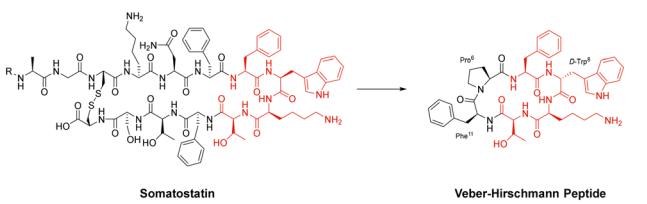

Fig. 7 Structural comparison between somatostatin and Veber–Hirschmann analogue.

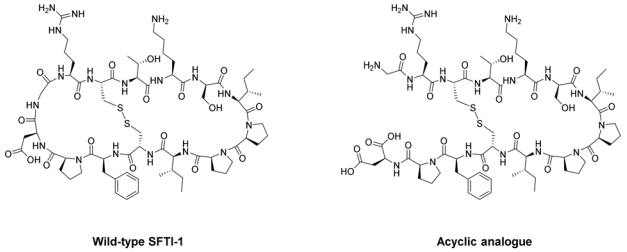

Fig. 8 Structural comparison between natural SFTI-1 and its acyclic analogue.

bridge.[84] Peptide cyclisations are generally carried out at high-dilution (<mM conc.) to promote intramolecular interactions and minimise troublesome intermolecular processes like polymerisation.

Macrocyclisation using SPPS has been employed as an effective means to generate cyclic peptides.[85] While the linear peptide is bound to the solid support (resin), it experiences a sort of pseudo-dilution phenomenon – where the functional groups bound to the resin are less likely to encounter one another in comparison to the free molecules within the solution. This environment promotes the favourable intramolecular interactions necessary for peptide cyclisation. To achieve on-resin cyclisation, the linear peptide is usually bound to the solid support *via* the side-chain of one of the amino acids in the sequence (*e.g.* Asp or Glu). At least 3 independent and orthogonal protecting groups (resin

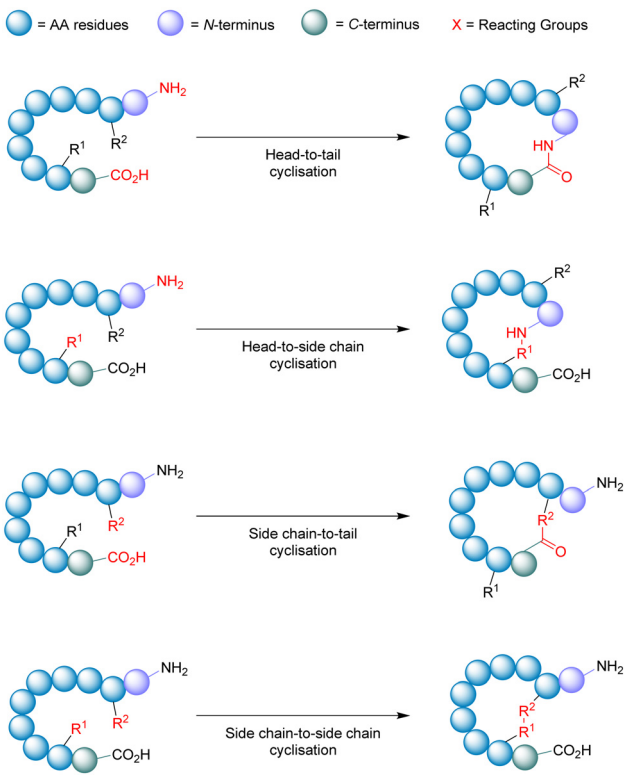

Fig. 9 Schematic illustration of cyclisation strategies.

included) are required for this strategy. The linear peptide needs to be constructed, N- & C-termini to be deprotected, cyclised from head-to-tail, and then finally cleaved from the resin.[86] A noteworthy feature of on-resin cyclisation is that basic washing and filtering is usually sufficient to achieve (relative) purity, circumventing intermediate purification steps and solubility issues.

One of the most important factors that influence the success of peptide cyclisation is ring size. The cyclisation of large peptides is sometimes reported as troublesome, however peptides containing >7 amino acid residues usually cyclise without too much difficulty. This is not the case for smaller peptide structures. During the head-to-tail cyclisation of peptides with <7 amino acid residues, C-terminal epimerisation and cyclodimerisation are common pitfalls.[87]

The activation free-energy ($\Delta G^{\ddagger}$) of cyclisation is governed by an enthalpy term ($\Delta H^{\ddagger}$) and an entropy term ($\Delta S^{\ddagger}$): $\Delta G^{\ddagger} = \Delta H^{\ddagger} - T(\Delta S^{\ddagger})$. Using the head-to-tail cyclisation approach as an example, the activation entropy ($\Delta S^{\ddagger}$) of the intramolecular interaction is based on the probability that the N- & C-termini approach each other at an angle (~107°)[88] to facilitate conjugation. This probability is reduced as the amino acid chain gets longer. One might assume that this should be of benefit to the smaller linear peptides (<7 AAs), however the loss in entropy is almost completely eclipsed by the enthalpic term. The activation enthalpy ($\Delta H^{\ddagger}$) represents the stress on the molecule during the transition state (‡). This value can be very high for peptides containing less than 7 amino acid residues, as there is significant ring-strain generated by the preferred confirmation of the amide bonds within – as all *trans*.[89]

One early study highlighted these challenges as they tried to synthesize numerous naturally occurring cyclic tetra- and penta-peptides using a head-to-tail style ring-closure. However, results were sparse with most cyclisation reactions proving unsuccessful.[90] They noted that the ring disconnection (site of cyclisation) had to be chosen very carefully, suggesting that product yields could be improved if the site of bond formation was not sterically hindered by the likes of *N*-alkylation or β-branched amino acids. They also documented improved macrocyclisation rates between two amino acid residues of opposite stereochemical configuration (D/L), and when linear peptides had a sufficient level of pre-organisation due to certain turn-inducing motifs. This study demonstrates the many difficulties that can arise from an apparently straightforward retrosynthetic analysis of cyclic peptides.

Conformational elements for cyclisation. Macrocyclisation is a fickle process that heavily relies on the ability of the linear peptide to adopt a conformationally pre-organised form that brings the two reactive groups within close proximity to one another before ring-closure. The need for adequate spatial proximity has been well-documented since 1963,[91] resulting in less by-products from intermolecular reactions. Achieving this spatial proximity is one of the main challenges associated with macrocyclisation, because of linear peptides' preference for adopting elongated conformations to reduce allylic strain.[92] This spontaneous process usually puts the reactive groups quite a distance away from each other. There are two main strategies used to counteract this problem: the first focuses on the internal conformational elements, which exploit covalent modifications of the peptide backbone to promote cyclisation. The second strategy utilises molecular scaffolds and template-mediated techniques to facilitate macrocyclisation.

Internal conformational elements. As mentioned above, peptide cyclisation is more successful when the linear peptide can accommodate the angular criteria for both reactive groups being in the transition state with the least amount of strain. Smith and Daidone studied this idea and demonstrated that the cyclisation rate of longer polypeptide chains is influenced by the formation of intra-peptide hydrogen bonds. This generates ephemeral β-sheet like structures that serve to lower the free-energy of macrocyclisation.[93] The inverse is also true, slower cyclisation kinetics are observed with the absence of these hydrogen bonds in smaller peptides. Peptides with few amino acid residues lack the structural flexibility to accommodate these intra-peptide formations, thus highlighting their inherent rigidity and reluctance towards cyclisation.

In order to optimise the macrocyclisation of peptides, chemists have yet again sought inspiration from nature to help them overcome their synthetic woes. The secondary structure of proteins – notably, the reverse turn – has inspired the introduction of a *cis*-amide bond in the middle of the peptide sequence.[94] This modification is analogous to a β-turn and provides an elegant way of obtaining sufficient spatial proximity between the reactive groups. Proline has the highest natural occurrence within these reverse turns, with the *cis*-amide bonds of proline (Fig. 10) being displayed in the crystal structures of many proteins. One classical study took advantage of this fact in the cyclisation of the tri-peptide cyclotri-L-prolyl.[95] In a similar fashion, linear precursors containing a di-proline unit with alternating stereochemistry (L-Pro-D-Pro or *vice versa*) are solid candidates for macrocyclisation due to their impressive β-hairpin inducing features. Robinson & group exploited this to generate cyclic peptides that accurately mimicked canonical

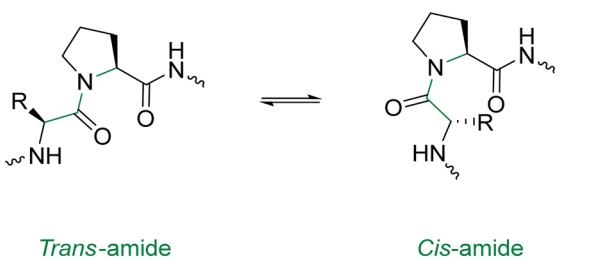

Fig. 10 *Cis & trans* proline isomerisation around the Xaa–Pro amide bond.

conformations of hypervariable loops observed in the crystal structures of antibody fragments.[96]

N-Methyl AAs have a comparable stereochemical influence on the backbone of peptides to that of the Pro residue. They can also be used to introduce *cis*-amide bonds into the peptide backbone and are well-equipped to generate β-turns.[97] Turn-inducing effects are not exclusive to the Pro residue. Indeed the incorporation of other D-AAs in to L-homopeptides can apply similar contortions, and have been used to improve the yields of several peptide macrocyclisations.[98,99]

External conformational elements. External elements for promoting peptide cyclisation operate by pseudo-isolating the linear peptide from the bulk solution. This unique micro-environment serves to reduce the chances of polymerisation or cyclo-oligomerisation.[100] Metal ions offer a non-covalent ancillary-based strategy for peptide macrocyclisation.[101] The inspiration for this strategy comes from the well-documented capability of cyclic peptides to act as ionophores – binding metal cations in solution and *in vivo*.[102,103] Beck and Co. were one of the first groups to demonstrate linear peptide pre-organisation *via* metal ions for the use of macrocyclisation.[104] They constructed a cyclic tetra-peptide through a metal-cation-assisted dimerisation of 2 dipeptide methyl esters under basic conditions (Scheme 1). An interesting caveat for this double head-to-tail lactamisation is that both dipeptides must orientate themselves in a *trans* fashion around the metal centre before nucleophilic attack can occur. This macrocyclisation strategy can facilitate ring sizes of 12- to 18-membered cycles, can incorporate α- and β-AAs, and does not require protecting groups, coupling reagents, or high-dilution conditions. The cyclic peptide product can then be purified *via* isolation of the coordinated dianion, and the metal ion can be liberated by acid methanolysis.

An analogous strategy – one that remains underdeveloped and largely unexplored – is the anion templation strategy. Although published reports on this strategy remain scant,[105,106] its use suggests that not only cations, but anions can be used for the pre-organisation of linear peptides to promote macrocyclisation. Speranza and Tomišić demonstrate this by using the Cl^- anion as a templating agent for the synthesis of cyclic peptides (Fig. 11).[107] They prepared 3 novel cyclic homo-lysines and 6 other cyclic peptides using the head-to-tail lactamisation strategy. Experimental yields of cyclic peptide products – that were Cl^- anion templated – were found to be significantly higher than those obtained *via* the cation approach. Indeed, in some instances, only the anion-mediated synthesis yielded the target cyclic peptides. To further support their theory that the Cl^- anion played a major role in the macrocyclisation reaction, they studied the corresponding ring-closure reaction kinetics. Macrocyclisation experiments were conducted using increasing concentrations of TEACl (2–100 eq.), with higher concentrations of TEACl inducing faster cyclisation rates and increased yields. This was evidenced by TLC and quantitative ^{1}H NMR analysis.

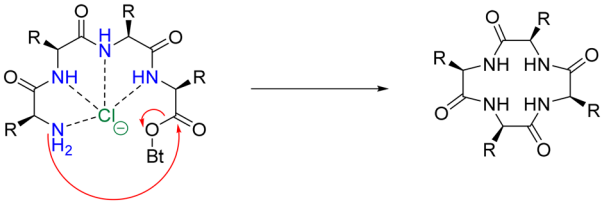

Fig. 11 Suggested mechanism for the chloride-mediated macrocyclisation (adapted from ref. 107 with permission from American Chemical Society, copyright 2020).[107]

It is understood that anion-recognition by cyclic peptides has been well-documented,[108] and many examples exist of their use as templating-agents for the synthesis of organic and inorganic scaffolds,[89,109] however – at the time of writing this – no example(s) of chloride-templated synthesis of cyclic peptides have been reported. This novel strategy for pre-organisation of linear peptides may promote further research into this vastly under-appreciated method of macrocyclisation. Peptidomimetic alterations of natural peptides can produce bio-active analogues. Furthermore, macrocyclisation of linear peptides is often used as an effective strategy to provide increased conformational rigidity and more bio-stable products.

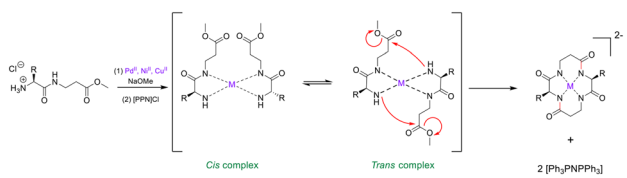

Scheme 1 Transition metal-assisted cyclo-dimerisation of dipeptide esters (adapted from ref. 104 with permission from John Wiley and Sons, copyright 1998).[104]

Substitution of L-amino acids with D-amino acids

Specific nomenclature has been used to denote the absolute configurations of the 4 substituents around sp^3 carbon atoms. The same notation is used for simple sugars and amino acids – the L- and D-system of absolute configuration(s), suggested by Emil Fischer.[110] He denoted chiral molecules with a configuration related to that of L-glyceraldehyde – L, while stereoisomers related to D-glyceraldehyde were described as D. It is also worth mentioning that not all L-AAs rotate plane-polarised light to the left, they can also rotate it to the right; and the same holds true for D-AAs. Fischer's notation, L- and D-only refer to the absolute configuration of the substituents about the carbon atom.

D-AAs, the enantiomers of the canonical L-AAs, came under investigation in the mid-20th century, prompted by Krebs' discovery of D-AA oxidase.[111] However, the use of D-AAs to improve proteolytic stability was not employed until much later. Zisman and Seia showed us that the incorporation of

D-AAs into polypeptide antigens could enhance their proteolytic stability.[112] Building on this work, Tugyi *et al.* studied the antigenic properties and proteolytic stability of certain MUC2 peptides partially substituted by D-AAs. Their goal was to generate peptides that were resistant to enzymatic degradation while possessing similar, if not increased, binding kinetics compared to the original L-homopeptides.[113] The results generated from this study suggested that the activity of the peptides was sustained even in the presence of 2 D-AA residues at its N-terminal flanking domain, and up to 3 at its C-terminal flanking domain. This novel D-/L-heteropeptide also displayed enhanced proteolytic resistance in lysosomal media and diluted human serum. These observations seem to demonstrate the benefits of appropriate D-AA modification(s) to produce synthetic antigens with comparable recognition properties and resistance to proteolytic degradation.

An interesting study by Werner *et al.* explored the effect(s) of heterogeneous-backbone modification for enhancing proteolytic protection. They employed the four most common motifs for this kind of modification: D-AA residues, N-Me residues, C_α-Me residues, and β^3 residues. From this, the group synthesized a family of compounds – 32 analogues of a control peptide – with residues replaced by the above mentioned motifs.[114] These heterogeneous-backbone motifs have already been studied in isolation,[64,115] but what makes this report exciting is that it has ventured to compare and contrast their ability to protect the substrate from proteolytic attack. Interestingly, the team discovered that the level of protection was as follows: D-AA > C_α-Me > β^3 > N-Me. D-AAs and C_α-Me residues induced proteolytic stability by moving the overall structure away from a conformation that was easily recognised by the enzyme. This imparted a large degree of proteolytic protection, with wide-ranging and synergistic effects when substitutions were combined in a single sequence. N-Me AAs were observed to influence proteolytic stability through the disruption of particular enzyme–substrate points of contact, with limited effect to local folding – resulting in short-range effects of humble magnitude, that were only additive when used in tandem. The protection offered *via* β^3 AAs was rather intricate – imparting only middling levels of stability, yet far-reaching. The authors describe the effects of combined β^3 replacement as partially-synergistic, but noted that the quantity of β^3 AAs did not directly correlate to enzymatic resistance.

Caution is advised when appropriating these findings in a more general sense, as the results generated by the group come from one single serine protease (chymotrypsin). Nonetheless, the study presents a solid hypotheses that will aid the future development of novel peptides/proteins containing enhanced proteolytic stability with minimal unnatural backbone content. D-AA residues possess folding characteristics that differ greatly from their L-AA brethren, this makes them rather effective turn-inducers. Building on the results highlighted in this study – demonstrating the ample proteolytic stability imparted by D-AAs – they may well be ideal candidates for bio-compatible backbone modifications.

Peptide conjugates

The original design of molecular conjugates can be attributed to the German physician/scientist Paul Ehrlich when he introduced us to the iconic phrase 'magic bullet'. This magic bullet is described as a cytotoxic payload that would only become armed when selectively delivered to the site of interest by a targeting motif.[116] It wasn't until 1958 when the first few examples were reported,[117,118] and only in 1983 did the first clinical trial of such a conjugate begin.[119] Fast forward another 20 years until the first FDA-approved conjugate (gemtuzumab ozogamicin) – operating under the trade name Mylotarg™ – consisting of an antibody bound to calicheamicin for the treatment of acute myeloid leukaemia.[120]

The conjugation of molecular species to peptides is an elegant strategy to tackle substandard aqueous solubility, premature metabolic degradation, and may also be used to promote cellular uptake. Certain peptide sequences can provide targeted-delivery of small molecules to boost local drug concentration. This in turn, helps to reduce the adverse effects pertaining to systemic exposure and from accumulation in healthy tissues.[121] Drug-conjugates that possess peptide carriers can bind to cell-surface receptors with high affinity – similar to that of antibodies – and recognise a whole host of endogenous targets. Clinically, the most famous of these biological receptors are the integrins, tyrosine kinases, and G-protein-coupled receptors. Peptide conjugates have a much smaller molecular size compared to antibodies, and may provide a more efficient delivery to obscure biological targets with decreased immunogenicity.

The pharmacokinetic profile of peptide–drug conjugates is unique, with a shortened circulation time and metabolic half-life in comparison to antibodies. This inherent property gives peptide-based drug conjugates an edge when it comes to the delivery of cytotoxic agents where prolonged exposure is undesirable. However, a significant drawback is encountered when dealing with solid tumours. Treatment of this nature usually requires long-lasting pharmacokinetics, often displayed by antibodies. Nowadays, as peptide chemistry has matured and improved, techniques such as pegylation, lipidation and other modern advancements has made up the difference, making them much more comparable to antibodies in this respect. The peptide–drug conjugate strategy has the potential to simplify commercial synthesis, streamline compliance with regulatory agencies and consequent criteria during manufacturing, and is a powerful means to achieve preferable disease outcomes that can be conveniently administered at a reasonable price.[122]

Linker and conjugation chemistry

The linker is an essential component of the peptide–drug conjugate strategy, and serves to covalently unite the peptide

and the small-molecule moiety. The linker supports both the peptide sequence and the payload (drug) by upholding their structural integrity during administration, until such a time when the conjugate has reached its desired destination. To reduce the likelihood of unwanted side-effects, it is desirable for a peptide–drug conjugate to have a linker that only releases the payload after the target (cancer cells *etc.*…) has taken up the conjugate intracellularly. However, upon systemic administration – most linkers within peptide conjugates start to break down quickly after being exposed to the blood plasma. The remnants of the intact-conjugate(s) are eventually taken up by the target cells, but this vastly diminished concentration can often prove inadequate.[123]

The linker within peptide–drug conjugates (usually) makes two covalent chemical bonds – one between the peptide/substrate and the linker, and another between the payload and the linker. The bond between the payload and the linker should be cleaved to release the free (unmodified) payload at the target site, and the bond between the peptide and the linker should not interfere with the peptide's affinity for its receptor. Many linker functional groups exist in the literature.[124] However, it is generally accepted that they can be arranged into 4 main families: acid-cleavable (carbonate & hydrazone), enzyme-cleavable (carbamate, amide & ester), non-cleavable (oxime, triazole & thioether), and reducible disulfide (Fig. 12). This (rather broad) categorisation was established by monitoring how these functional groups reacted after cellular uptake or in the presence of *in vivo* stress. Because of this, linker chemistry can often dictate whether or not the overall conjugate will be successful in enhancing efficacy. This section will provide a brief summary of the main linker strategies used in the design and synthesis of peptide–drug conjugates, with a focus on enzyme-cleavable linker chemistries.

Linker chemistries that involve enzyme-cleavable amide or ester bonds have become attractive, as they can be manipulated for site-specific cleavage in lysosomes or tumour microenvironments. Cancer cells' intracellular compartments – such as lysosomes and endosomes – have high levels of esterases and amidases, which can be utilised for site-specific release through upregulated expression of these enzymes. More complex amino acid sequences recognised by enzymes like caspase-3 or cathepsin B have been employed as linkers.[125,126] It is important to note that these enzyme-cleavable linker chemistries are not foolproof, as many accidental-cleavage opportunities can arise prior to reaching the intended target. Appropriate control of the linker chemistry is essential for ensuring the overall stability of the conjugate until it reaches the target site.

Ester & amide. Ester and amide functional groups are commonly used in linker chemistry to covalently bind different molecular entities – such as drugs or targeting moieties – in a conjugate. Ester linkers, which are cleaved by esterases, are often used to achieve a controlled release of the drug/payload. Amide linkers, on the other hand, are generally more stable and resistant to hydrolysis. This makes them suitable for constructing conjugates with enhanced stability, or for creating prodrugs that require metabolic activation. The choice of linker and functional group can have a significant impact on the pharmacokinetics and efficacy of the conjugate.

One study employed an ester bond to couple paclitaxel to a peptide called angiopep-2. In this peptide–drug conjugate, the paclitaxel molecules are coupled to the side-chain(s) of two Lys residues and the N-terminal amine of angiopep-2, to form the complete therapeutic (Fig. 13).[127] This conjugate (ANG-1005) is currently being used for treating patients that display solid tumour or brain metastasis. It works by overcoming the main drawback of (unmodified) paclitaxel, which struggles with blood–brain barrier permeability due to the presence of multi-drug resistance efflux pumps in brain tumour cells. The ester bond of the peptide–drug conjugate is selectively cleaved by esterases within the lysosomes, delivering paclitaxel to the brain.

A radionuclide coupled to the peptide octreotide – called ^{177}Lu DOTA–TATE (Lutathera®) – was approved by the FDA in 2018 for treatment against neuroendocrine tumours (targeting somatostatin receptors).[128] ^{177}Lu DOTA–TATE is administered during peptide-receptor radionuclide therapy (PRRT) – a type of internal radiotherapy, also known as radioligand therapy – and was the first peptide–drug conjugate to be approved by the FDA for treating prostate

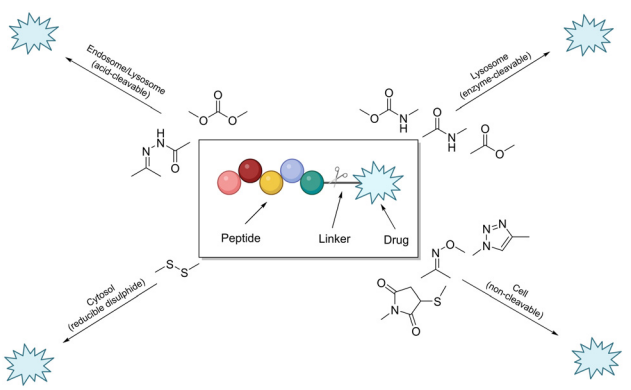

Fig. 12 Cartoon schematic of a peptide–drug conjugate, and the associated linker chemistries (adapted from ref. 123 with permission from American Chemical Society, copyright 2021).[123]

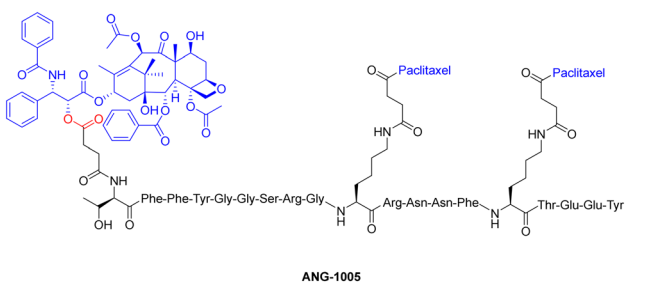

Fig. 13 Chemical structure of paclitaxel conjugate ANG-1005 (ester bond highlighted in red).

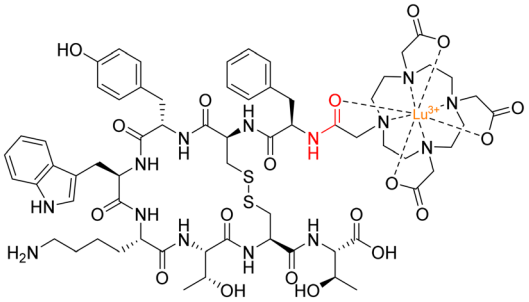

Fig. 14 Structure of ^{177}Lu DOTA–TATE with amide bond highlighted in red.

cancer.[129] This conjugate consists of the radionuclide ^{177}Lu chelated to 1,4,7,10-tetraazacyclododecane-1,4,7,10-tetraacetic acid (DOTA), and DOTA is coupled to Tyr$^{(3)}$-octreotate (TATE) by an amide bond (Fig. 14).[130]

To maximise effectiveness, ester and amide linkers need to be carefully manipulated so that they remain inert until within the tumour tissue/cancer cells. Although research in this area has boomed in recent years, more data is needed to understand what specific manipulations of amide/ester linkers can be employed to enhance chemical stability and efficacy.

Carbamate. Peptide–drug conjugates can also utilise the carbamate functional group to fortify their structure. The carbamate linker can be cleaved by particular enzymes present within intracellular endosomes or lysosomes.[124,131] One study (again) focused on synthesising peptide–paclitaxel conjugates using carbonate or carbamate linker chemistries, with the peptide getting selectively cleaved by the prostate-specific antigen (Fig. 15). Evaluation of these peptide–drug conjugates demonstrated that compounds possessing the carbamate linker were more stable than their carbonate analogues.[132] Furthermore, these carbamate conjugates had the desired stability for specific release of the payload in the presence of prostate antigens, thus proving fatal to the prostate cancer cells.

This study agrees with other reports that suggest the *in vivo* linker stabilities can be ranked as follows: amide > carbamate > ester > carbonate.[133] However, further studies are required to demonstrate which linker strategy will lead to better efficacy for tumour reduction.

Dipeptide & tripeptide. A different approach demonstrates the use of specific di- and tri-peptide sequences for the

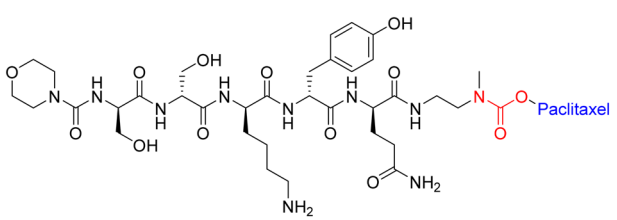

Fig. 15 Example of peptide–paclitaxel conjugate with carbamate bond highlighted in red.

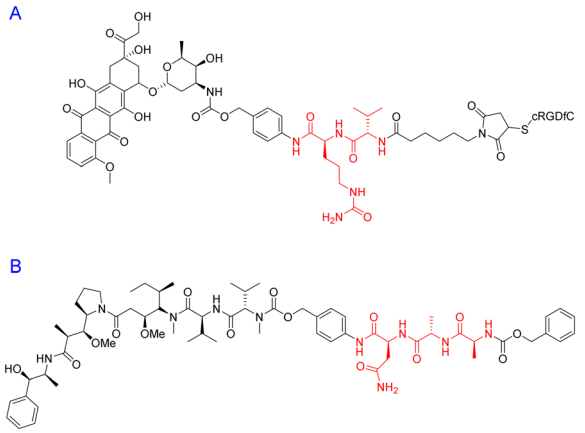

Fig. 16 Peptide–drug conjugates with (A) di- and (B) tri-peptide linkers highlighted in red.

controlled release of drugs from peptide–drug conjugates. The group of Liang and Co. synthesized compound A (Fig. 16), containing the linker di-peptide – Val-Cit – for targeted cleavage *via* carboxypeptidase (cathepsin B). In this study, the group seeks to compare the antitumor efficacy of peptide–doxorubicin conjugates by varying covalent linkers strategies.[134] Di-peptide A is covalently bound to doxorubicin by a *para*-aminobenzyl carbamate (PABC) spacer which experiences a spontaneous electron-cascade *via* a 1,6-elimination upon enzymatic degradation of the C-terminal (amide) Cit-residue. The authors acknowledge that the linker chemistry takes inspiration from a currently FDA-approved antibody–drug conjugate (ADC) called brentuximab vedotin (Adcetris®). The Val-Cit sequence is cleaved by cathepsin B – which exists in abundance within the lysosomes of tumour cells – leading to site-specific payload release. The results of this investigation concluded that compound A displayed enhanced cytotoxicity towards tumour cells, increased cellular uptake, and superior *in vivo* efficacy (mice) when compared to other peptide–drug conjugates with different linker functionalities.

The tri-peptide sequence has also been used for the site-specific release of payloads within tumour micro-environments. Ala-Ala-Asn is a cleavable sequence that undergoes degradation *via* the enzyme legumain.[135] The asparaginyl endopeptidase – legumain – is reported to be upregulated in tumour cells and specifically cleaves at the C-terminus of asparagine.[136] One group was determined to capitalise on this catalytic property for prodrug activation – with potential application(s) in cancer therapy. To this end, Bajjuri and colleagues synthesized distinct prodrugs containing the cytotoxic payload(s) monomethylauristatin E (MMAE) or didesmethylauristatin E (DDAE) conjugated to the tri-peptide (B) *via* an amide or carbamate bond (Fig. 16).[135] The absence of a targeting peptide within their synthetic design is noted, however these novel prodrugs display considerable synthetic flexibility and could potentially be functionalised with a specific peptide sequence to enhance their site-specificity. Among the Bajjuri-prodrugs that were

synthesized, compound B was found to yield the best results, demonstrating 57% inhibition (4T1 breast cancer) in mice when compared to subjects treated with buffer alone. Interestingly, tri-peptide prodrug B managed to overcome one of the main drawbacks of MMAE-based therapeutics, displaying no cytotoxicity, in contrast to the high mortality rate observed in mice that were treated with MMAE alone.

The selection of both the linker and functional group holds significant importance in peptide–drug conjugates, as it profoundly impacts the intended pharmacokinetic and pharmacodynamic characteristics of the conjugate. Notably, factors such as linker length, composition, and flexibility play a pivotal role in governing the conjugate's stability, the pace of drug liberation, and its elimination rate from the system. Moreover, the functional group present on the linker exerts an influence on enzymatic breakdown and cellular absorption of the conjugate, thereby ultimately shaping its effectiveness and safety profile.

Convergence of therapeutics and sensing

Peptide probes with luminescent sensing capabilities are used throughout the chemical and biomedical fields. In cellular imaging, these probes allow real-time visualisation of biological processes without disrupting cellular functions, while also enabling molecular recognition and selective binding to specific biomolecules.[137] This aids in disease diagnosis and monitoring, particularly in biosensing applications for early detection of diseases like cancer. Moreover, luminescent peptide probes play a vital role in drug development through high-throughput screening and target validation, expediting the identification of potential therapeutic agents.[138]

Fluorescent peptide probes

The fields of chemical diagnostics and imaging are constantly being developed and updated, with fluorescence imaging becoming an essential technique for observing changes in biomarkers within living systems.[139,140] The compounds that generate fluorescent-imaging data are called – fluorogenic probes. These latent fluorophores can modulate their signal in response to environmental fluctuations, analyte interactions, or chemical modifications.[141] Fluorogenic probes are synthesized by chemically engineering the parent probe so that its fluorescence profile is sufficiently distinct from the released fluorophore – this activation is usually triggered by a specific event. In the interest of conciseness, this specific introductory section will focus solely on enzyme-activated fluorogenic probes. For more information regarding fluorescent spectroscopic properties and fluorophore chemistry, see the following papers discussed elsewhere.[142,143]

Enzyme-activated fluorogenic probes that take advantage of enzymatic degradation to modulate fluorescence output, can equip researchers with an impressive toolkit for monitoring biological events *in cellulo* and *in vivo*. Initially, many enzyme-activated probes were constructed around xanthene dye motifs, for the detection of esterases,[144] galactosidases,[145] lipases,[146] and phosphatases.[147] Building on from this work, primitive live-cell imaging was possible *via* cell-permeable probes,[148] paving the way for more advanced fluorometric applications, including enzyme-linked immunosorbent assays (ELISAs),[149] diagnostic tests,[150] and viability assays.[151] Advancements in the design of fluorogenic probes are constantly stimulating the progress of complementary methodologies and their practical applications in the field of chemistry.

The two main strategies employed for fluorogenic probe design and application are; the latent properties of the fluorophore itself, and the method utilised to hide its fluorescence. Some crucial properties of the parent fluorophore may include; excitation and emission wavelength(s), resistance to photobleaching, quantum yield, and effects of pH on fluorescence output. Recently, researchers have begun to focus their attention on generating fluorogenic probes that do not overlap with auto-fluorescence produced by endogenous species, and result in minimal phototoxicity. Probes that fluoresce in the near-infrared and far-red region have an emission wavelength far above (nm) the auto-fluorescence window.[152,153] It is also worth noting that optimising the spectroscopic properties and brightness (product of quantum yield and extinction coefficient) is quickly becoming an essential part of the design strategy for the synthesis of fluorogenic probes.

D. Tang and coworkers have elegantly exploited the use of fluorogenic probes as a method for detecting carcinoembryonic antigen (CEA) using a bio-responsive release system (Fig. 17).

The group engineered an all-in-one paper-based analytical device (PAD) system that combined DNA-gated mesoporous silica nanocontainers with CdTe/CdSe quantum dots and enzymes on paper.[154] Glucose-loaded mesoporous silica nanocontainers with a CEA aptamer and CdTe/CdSe quantum dot-enzyme paper were utilised in a centrifuge tube for this assay, with the fluorescence of the quantum dot-enzyme paper becoming quenched at higher CEA concentrations.

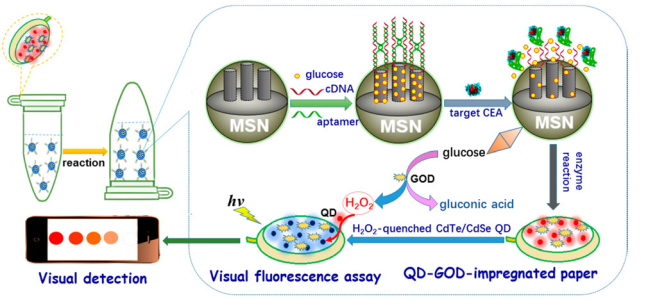

Fig. 17 Graphical illustration of the PAD for the visual fluorescence detection of CEA (reprinted from ref. 154 with permission from American Chemical Society, copyright 2017).[154]

This produced a colour change from red to colourless, which facilitated the qualitative evaluation of CEA levels visually, and quantitative determination *via* a fluorimeter.

A similar study by the same group investigated the NH_3-triggered structural change of NH_2-MIL-125(Ti) impregnated on paper, for the detection of CEA.[155] Gold nanoparticles were functionalised with glutamate dehydrogenase, and secondary antibodies were used to generate wet NH_3 in a sandwiched immunoassay format. The PAD coated with NH_2-MIL-125(Ti) showed good visible fluorescence intensity through wet NH_3-triggered structural change with high accuracy and reproducibility, indicating the device's potential for protein diagnostics and biosecurity.

The inherent properties of a fluorogenic probe are indeed important, however, the strategy used to mask its fluorescence will likely impact its enzymatic target and determine its effectiveness. An efficient fluorescence masking-strategy would see the probe generate a response selectively for the target enzyme, be chemically inert until within sufficient proximity, and terminate absorption and fluorescence output at the initial excitation wavelength (upon activation).

Fluorescence quenching techniques based on Photoinduced Electron Transfer (PET) and Förster Resonance Energy Transfer (FRET), and to a lesser extent – Ratiometric Imaging, have been very popular in recent years (Table 1).[159] Indeed, one interesting example involved a novel immunoassay strategy for detecting cancer biomarkers – focusing on alpha-fetoprotein (AFP) as a model analyte.[160] This method focused on the enzyme-controlled formation of fluorescent polydopamine (PDA) nanoparticles *via* the dissolution of manganese dioxide (MnO_2) nanoflakes. The *in situ* synthesis of PDA nanoparticles possessed high specificity and a low detection limit, indicating the potential of this "off → on" fluorescence strategy as a tool for early cancer diagnosis.

In contrast to this, an "on → off" fluorescence quenching strategy has been employed for the detection of prostate-specific antigen (PSA), without interference from autofluorescence.[161] This study detailed the preparation of Mn^{2+}- & Pr^{3+}-doped Zn_2GeO_4 nanorods with persistent luminescence properties and their application as pH-responsive fluorogenic probes. The fluorescence intensity (533 nm) was observed to decrease with increasing concentrations of PSA, which was verified by control experiments, optimization of experimental conditions, and analytical performance evaluation with PSA standard samples. Overall these studies highlight the potential of fluorescence quenching techniques to produce novel and innovative nanomaterial sensing systems.

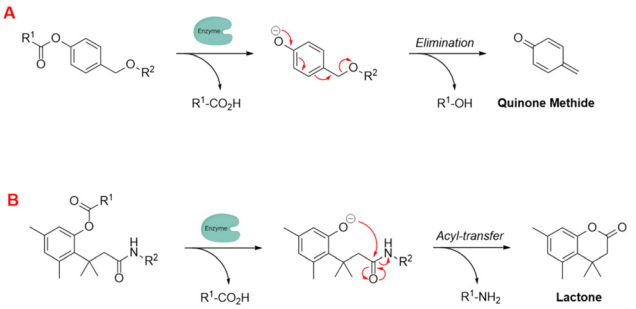

Fig. 18 Examples of self-immolative linker strategies – mechanism(s) of activation, (A) elimination and (B) acyl-transfer (adapted from ref. 164 with permission from American Chemical Society, copyright 2018).[164]

To further enhance these quenching techniques, self-immolative linkers have been employed to enhance probe stability and performance.[162] Dal Corso and Gennari described self-immolative linkers as "*covalent constructs designed to degrade spontaneously in response to a specific stimuli*".[163] The two most prevalent self-immolative linker motifs in literature (in regards to enzymatic probes) are elimination (electron cascade) and acyl-transfer (Fig. 18). In this particular context, the linker is being used to modify the fluorescence profile as a means for detecting the presence of a hydrolytic enzyme. It is worth highlighting that self-immolative linkers have demonstrated their utility in both peptide/small molecule and macromolecular drug-delivery and sensor systems. After additional refinement, these systems may have the potential to evolve into commercially feasible solutions.

In the next few sections, we will focus our attention on peptide-based fluorescent probes and build on some of the ideas that were discussed above.

Intrinsic peptide-based fluorescence. It is widely acknowledged that amino acids play a pivotal role as vital nutrients in biological organisms. Consequently, functional

Table 1 Examples of fluorescence quenching techniques commonly exploited in fluorogenic probes[156–158]

Fluorescence quenching technique	Description
Förster Resonance Energy Transfer (FRET)	A non-radiative energy transfer between a donor fluorophore and an acceptor molecule
Photoinduced Electron Transfer (PET)	An electron is transferred from the excited state of the fluorophore to a nearby electron acceptor (quencher)
Internal-charge Transfer (ICT)	Involves the transfer of an electron or charge within a molecule
Through-bond Energy Transfer (TBET)	Involves the transfer of energy between two fluorophores linked by a series of covalent bonds
Aggregation-induced Emission (AIE)	Fluorescence enhancement upon aggregation – often associated with restricted intramolecular motions within the luminogenic molecule

Table 2 Fluorescent properties of 3 natural aromatic AAs[168,169]

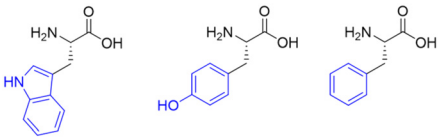

	Tryptophan	Tyrosine	Phenylalanine
$\lambda_{ex}/\lambda_{em}$ (nm)	220/360	225/304	220/285
Absorptivity (ε) (L mol^{-1} cm^{-1})	5600	1400	200
Lifetime (τ) (ns)	3.1	3.6	6.4
Quantum yield (Φ_F)	0.2	0.14	0.04

materials crafted from naturally occurring amino acids exhibit commendable biocompatibility and environmental friendliness. The aromatic amino acids, including tryptophan, tyrosine, and phenylalanine, possess inherent fluorescence properties (Table 2), rendering them suitable candidates for developing peptide-based fluorescence probes.[165] To date, numerous such probes – utilising these aromatic residues – have been documented in the literature.[166,167]

One popular use of these aromatic residues is in the study of self-assembling peptides – employing the endogenous fluorescence as a marker. The fluorescence data may be used to probe the conditions necessary for the covalent synthesis of the peptide itself,[167] or to investigate the compound's effect on the micro-environment – by creating self-assembling peptides with fluorescence output that can be altered under different conditions.[170] In the context of peptide conformational changes, the accumulation and internal clustering of amino acids within peptides can induce structural modifications, and may potentially influence the fluorescent characteristics of the peptides.

An interesting facet regarding the Trp residue is that the native peptide-bond can act as a weak intermolecular quencher for the fluorescent indole moiety, which is further enhanced (quenching ability) in cyclic peptides.[171] In the case of Tyr fluorescent peptides, the tyrosine kinase protein plays a significant role in influencing peptide fluorescence, as it can induce phosphorylation of Tyr residues within peptides, resulting in the suppression of intrinsic fluorescence.[172] Fluorescent peptides containing the Phe residue can be used for monitoring the *in vitro* interactions with circulating-tumour DNA.[173] This interaction can cause the fluorescence output of the Phe residue(s) to become quenched, and may provide a novel method for DNA detection.

Peptide fluorescence *via* coupled fluorophore. As we have discussed above, the Trp, Tyr and Phe residues are inherently fluorescent, thus, making them potential candidates for naturally occurring fluorophores. However, some of their optical properties can be problematic, such as their low (high energy) excitation and emission wavelengths, poor brightness and photostability – making them substandard for many biological assays. The most popular fluorophore among the natural aromatic amino acids – tryptophan, absorbs and emits in the UV region and its fluorescence quantum yield is roughly 20% (Table 1). Researchers have tried to improve the fluorescent properties of tryptophan, with initial attempts involving aza-tryptophans as potential isosteric analogues in proteins,[174] and cyano-tryptophans – which possess quantum yields approaching 50%.[175]

Despite significant advancements in the development of probes utilising canonical aromatic amino acids to generate fluorescence data, the covalent combination of fluorescent moieties offers an alternative and effective approach for producing peptide structures with tuneable and enhanced optical properties. The synthesis of fluorescent peptides typically involves coupling the fluorophore to a reactive site within the peptide (side-chains, N-/C-termini or incorporated spacer), with initial coupling experiments targeting carboxylic acids, amides and thiols[176] – and more recently phenols[177] and imidazoles.[178] However, the covalent coupling of a fluorophore to a peptide can potentially disrupt and alter the properties of the peptide. Consequently, selecting an appropriate fluorophore is of utmost importance, as different fluorophores exhibit distinct chemical characteristics.

Many organic fluorophores available today possess a wide range of physico-chemical properties, which can impact biologically-active peptides (when coupled together). Antimicrobial peptides (AMPs) are compounds generated by various organisms, including fungi, protozoa, bacteria, plants, and animals as a natural defence mechanism against common human pathogens.[179] Functionalising these peptides with fluorophores has become a useful way for researchers to investigate their mechanism of action and design imaging probes for the swift detection of microorganisms at sites of infection.[180] AMPs have been modified to contain various synthetic handles (carboxylic acid, sulfonyl chloride, alkyne *etc.*…) to facilitate facile

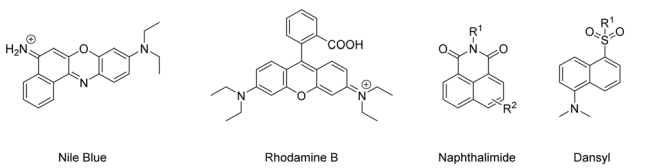

Fig. 19 Example fluorophores suitable for coupling to AMPs (counter ions omitted for clarity).

coupling with fluorophores without hindering their main identification characteristics.[181,182] A study by the Vendrell group sought to uncover the optimal fluorophore to label AMPs.[183] They found that certain larger fluorophores – like Nile blue and Rhodamine B – and smaller fluorophores – naphthalimide and dansyl – had little effect on their antifungal activity (Fig. 19).

Cell-penetrating peptides (CPPs) serve as efficient delivery carriers, and the investigation of their uptake and transportation mechanisms often involves the use of conjugates labelled with fluorophores.[184] Fluorophores tend to be (relatively) planar lipophilic molecules, with a rigid and bulky structure containing a (sometimes extensive) aromatic conjugated double-bond system. Many characteristics of CPPs (cellular uptake, membrane affinity, intracellular transport, and cytotoxicity) can be affected by the inherent properties of the fluorophore.[185] However, Birch demonstrated that CPPs coupled to fluorophores possess enhanced membrane association and display a more defined intracellular localisation pattern.[186] When choosing a fluorophore for conjugation with biologically active peptides found in organisms, it is essential to consider its potential toxicity and any adverse side-effects, as well as the fluorescence intensity it exhibits during its application.

Application(s) of fluorescent peptide probes. Peptides serve as exceptional scaffolds for biological investigations, given their ability to facilitate the precise monitoring of specific molecular interactions across a wide spectrum of biomolecules. The conjugation of a peptide to a fluorophore through covalent (bond formation) or other mechanisms not only preserves the inherent benefits of the peptide but also enhances the stability and longevity of the overall probe. In recent years, there has been a growing focus among researchers regarding fluorescent peptide probes, as they can be harnessed for the detection of tumour cells, metal ions, and various other substances. Consequently, the advancement of fluorescent peptide probes holds significant potential for expanding its application within the medical field.

Monitoring protein–protein and protein–DNA interactions. Many biological processes hinge on the interplay between proteins and their binding partners. Within this framework, fluorescent peptide probes have been constructed to gain deeper insights into protein-based interactions at the molecular level. For example, Sainlos engineered a phthalimide-based fluorescent peptide probe to explore the dynamic protein–protein interactions within the PDZ domain – one of the most prevalent protein-interaction domains in eukaryotes.[187] On a similar note, novel fluorogenic peptides have been employed as conformational reporters for calmodulin – a major calcium signal-transduction protein. Ito and coworkers first identified the calmodulin-binding peptides *via in vitro* selection using tRNA carrying a modified amino acid,[188] which was later improved (by the same group) with the addition of a 4-*N*,*N*-dimethylamino-1,8-naphthalimide (Fig. 20). This naphthalimide moiety possessed a similar emission wavelength (530 nm), however, it displayed a significantly improved fluorescence output (100-fold increase upon binding to calmodulin).[189]

Monitoring peptide–membrane interactions. Fluorescent peptide probes can also be tailored for investigating peptide–membrane interactions, which play a critical role in peptide-based therapeutics and transfection agents. Cationic peptides – like AMPs – show promise in this regard, owing to their ability to bind to membranes. Analogues of melittin – a major component of bee venom – containing a fluorescent modification on one (or more) of its 26 residues, has been synthesized by Postupalenko to investigate its orientation within lipid-rich membranes.[190] The group discovered that melittin aligns itself parallel to the surface of cell membranes. Analogous methods have been employed to investigate the membrane binding interactions of neuropeptides, which act as messengers between neurons.[191]

Real-time cell optical imaging. Optical microscopy has enabled researchers to observe the migration of biomolecules inside the cell with precise accuracy and high resolution. Fluorescent peptide probes are exceptionally well-suited for optical imaging, as they possess the ability to target specific proteins within cells and may incorporate optical reporters that can be readily detected through fluorescence microscopy. To aid the detection of pulmonary infections, Trp-BODIPY fluorescent probes were synthesized to visualise *Aspergillus fumigatus* in human lung tissue.[180] This modified residue serves as an ideal reporter due to its ability to maintain the molecular recognition properties of the native tryptophan while also offering a fluorescent output upon specific binding to fungal cells (Fig. 21). Additional fluorescent probes – containing antimicrobial peptides – have facilitated the real-

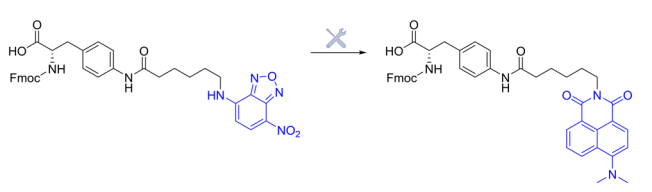

Fig. 20 Initial benzoxadiazole- *vs.* improved naphthalimide-based fluorogenic amino-acid.

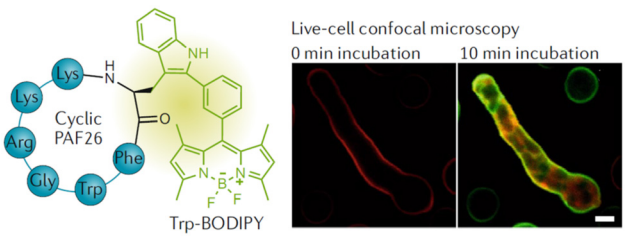

Fig. 21 Chemical structure of the Trp-BODIPY-labelled cyclic peptide and live-cell confocal imaging of *Aspergillus fumigatus* over time (reprinted from ref. 180 with permission from Springer Nature, copyright 2016).[180]

time, *in situ* detection of bacteria in excised human lungs through optical endomicroscopy.[192]

Optical imaging studies can also be conducted to obtain substance-related read-outs from cells. For example, fluorescent peptide probes containing coumarin-modified amino acid residues have been designed to report the endogenous phosphatase activity of protein tyrosine phosphatases in live cells.[193] The wash-free imaging capabilities of fluorescent peptide probes makes them valuable tools for applications where samples need to be analysed quickly with minimal processing steps, as seen in metabolic engineering and clinical diagnostics.

Lanthanide-based peptide probes

Luminescent lanthanide Ln^{3+} complexes – particularly those of Eu^{3+} and Tb^{3+} – have garnered significant attention in recent years owing to their unique photophysical properties and potential applications in fluoroimmunology, NIR-spectroscopy, and lighting devices.[194,195] This class of compounds exhibits narrow emission bands, long luminescence lifetimes, and resistance to photobleaching, making them promising candidates for use in biological imaging, sensing, and opto-electronic devices.[196] The prolonged luminescence lifetimes of emissive Ln^{3+} complexes facilitates the use of time-gated detection techniques (Fig. 22) to remove the inherent autofluorescence present biological fluorophores, thus enhancing the signal-to-noise ratio of the luminescence output.[197] Additionally, their ability to tune emission colours, and their high quantum yields make them an attractive alternative to traditional organic fluorophores.

Multiple factors must be taken into account when designing a luminescent lanthanide complex. First and foremost, it's important to note that directly exciting Ln^{3+} ions is highly inefficient, primarily due to the Laporte forbidden character of f–f transitions. Ln^{3+} ions in aqueous environments usually do not luminesce due to the efficient non-radiative decay process provided by the surrounding H_2O molecules. Nevertheless, the luminescent characteristics of lanthanides can be enhanced by chelating the ions with appropriately designed ligands that exhibit strong light-absorbing properties – antennae.[199] Ln^{3+} ions can therefore be shielded from the solvent environment, and the electronic energy in the form of light absorption from the ligands can be transferred to the metal ion. A cartoon schematic describing the photophysical pathway for Ln^{3+} luminescence is outlined in Fig. 22. This process involves an energy transfer from the excited state of an (appropriately) absorbing antenna to the Ln^{3+} excited state, which results in metal-centred luminescence.[200] The choice of the sensitising group can be especially valuable when creating responsive lanthanide probes, as alterations to the antenna can influence its absorption or energy transfer properties.

The next thing to consider is, Ln^{3+} ions generally maintain coordination numbers between 8–10 in aqueous environments,[201] so the synthesized ligand must be able to facilitate enough hard donors to complete this coordination sphere. There exists many kinetically stable Ln^{3+} complexes containing heptadentate or octadentate ligands, featuring; the carboxylic acid functionalised cyclen, EDTA, DTPA, and 9N3 macrocycles.[202,203] If the Ln^{3+} coordination sphere is not complete, H_2O molecules will coordinate to the remaining site(s). In this case, there may be a luminescence quenching event due to vibrational energy transfer to O–H oscillators.[204] This quenching effect of coordinated H_2O molecules can be used for the design of responsive Ln^{3+} complexes, where upon displacement of the coordinated water can lead to an increase in luminescence intensity.[194]

As we have seen before, amino acids/peptides possess diverse chemical functionalities, and can readily undergo functional-group interchange, with the introduction of groups such as aromatic rings, alkyl chains and heteroatoms. This diversity is valuable for creating peptides with specific

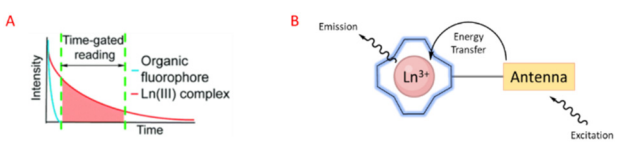

Fig. 22 Prolonged luminescence lifetime of the Ln^{3+} complex, in contrast to traditional organic fluorophores (A) (reprinted from ref. 198 with permission from Royal Society of Chemistry, copyright 2018).[198] Cartoon schematic of antenna excitation (B).

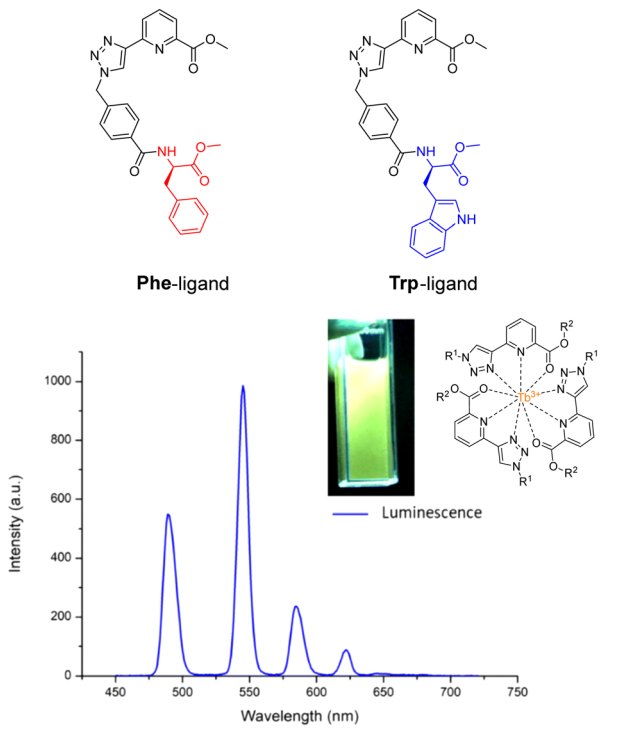

Fig. 23 Structures of ligands Phe & Trp, and the delayed luminescence spectra of $[Tb(Phe)_3]^{3+}$ recorded in MeCN. Inset: Picture of complex solution under illumination *via* UV lamp (adapted from ref. 205 with permission from Royal Society of Chemistry, copyright 2023).[205]

chemical, electronic, or steric characteristics. The Gunnlaugsson group elegantly exploited this idea with their recent publication detailing the synthesis of chiral α-amino acid derived ligands for Ln^{3+} luminescence.[205] These novel ligands contained L-phenylalanine and L-tryptophan – as their methyl esters – which underwent supramolecular self-assembly to form 1:3 complexes with Tb^{3+} under thermodynamic control. Indeed, both complexes were able to evoke Tb^{3+}-centred emission (λ_{ex} = 255 nm). Fig. 23 highlights the Tb^{3+}-centred transitions of complex $[Tb(Phe)_3]^{3+}$ at λ_{max} = 490, 545, 584, 622, 648 and 645 nm, upon deactivation of the $^5D_4$ state to the ^7F_x (x = 6–2) states, respectively.

Although the Tb^{3+} coordination sphere was populated by the (1,2,3-triazol-4-yl)-picolinamide motif and did not involve the C-terminal amino acid(s), this functionality may act as a site for further conjugation chemistry. For example, in the production of soft-materials, where the acid-moiety could be used to extend the overall supramolecular assembly.

Coupling lanthanide complexes to peptides and proteins. The integration of lanthanide complexes into peptides and proteins represents a vibrant area of ongoing research, and will be discussed throughout this section. Tagging peptides and proteins with Ln^{3+} ions most often involves the coupling of a stable Ln^{3+} complex to the amino acid residues.[206] Similar approaches using traditional fluorophores are widely employed in the development of various biological assays for studying ligand binding and enzyme activity. Lanthanide-based peptide probes have been predominantly utilised for monitoring phosphatase and kinase activity.[207]

An early example of a lanthanide-based peptide probe employed a simple DTPA ligand coupled to dipeptides Ser-Trp and phospho-Ser-Trp – utilising the Trp residue as an antenna. Tremblay and coworkers discovered that Tb^{3+} luminescence was enhanced by the non-phosphorylated (Ser-Trp) ligand, in contrast to the phosphorylated ligand.[208] This phenomenon was ascribed to a transition from a monomeric state to a dimeric state, which occurs in the phosphorylated and non-phosphorylated peptides, respectively. This change in luminescence output was employed to track the enzymatic dephosphorylation of the phosphorylated peptide using alkaline phosphatase. Tremblay developed this idea further by using a non-canonical quinolone antenna, and inserting an isoleucine residue between this new antenna and the phosphor-Tyr amino acid. This novel peptide-probe facilitated Eu^{3+} and Tb^{3+} luminescence upon phosphorylation (Fig. 24), and was applied to observe the conversion between non-phosphorylated and phosphorylated peptides using tyrosine kinase or tyrosine phosphatase.[209]

A lanthanide-based peptide probe containing a DO3A-propylamino ligand was coupled to an aspartic acid residue (resin bound), using typical Fmoc SPPS.[210] Interaction from a nearby phospho-Ser residue induced competitive displacement of the β-diketonate antenna from the Eu^{3+} coordination sphere, causing a subsequent decrease in Eu^{3+} luminescence output (Fig. 24). This "on–off" change in luminescence was utilised to monitor PKCα-catalysed phosphorylation of the peptide, with the aim of generating Michaelis–Menten kinetic data for the enzyme. On the other hand, the dephosphorylation pathway could be monitored by observing the enhancement in Eu^{3+} luminescence intensity upon preferential coordination to the β-diketonate.

The Arg-Gly-Asp (RGD) tripeptide motif displays a high affinity for the $\alpha_v\beta_3$ integrin – which is often associated with tumour metastasis.[211] Out of numerous RGD-containing structures, the c(RGDfV) peptide – originally synthesized by Kessler and colleagues in 1992 (ref. 212) – stands out as a remarkably potent and selective $\alpha_v\beta_3$ antagonist.[213] This cyclic-pentapeptide sequence has since become a well-established vehicle for targeted drug-delivery and cancer imaging.[214,215] Indeed, Gillaizeau and coworkers utilised it as a benchmark to showcase the efficacy and versatility of their design strategy.[216]

The group employed this cRGD-peptide – as a targeting agent – in a methodological attempt to generate NIR-imaging probes, by combining a DO3A-based ligand and an

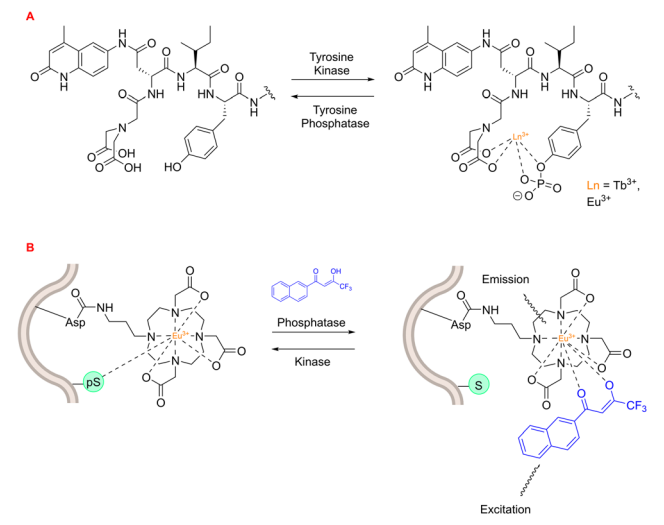

Fig. 24 Lanthanide-based peptide probes to monitor enzyme activity. (A) Observing tyrosine phosphatase and kinase activity using a 5-residue peptide (adapted from ref. 209 with permission from American Chemical Society, copyright 2008).[209] (B) Asp-functionalised Eu^{3+} complex within peptide sequence coordinates to phospho-Ser residue (adapted from ref. 210 with permission from Royal Society of Chemistry, copyright 2012).[210]

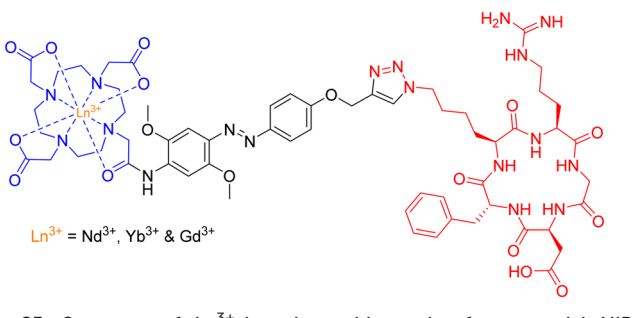

Fig. 25 Structure of Ln^{3+}-based peptide probe for potential NIR cancer-imaging.

azobenzene-antenna to promote lanthanide luminescence (Fig. 25).

Photophysical evaluation of this design strategy demonstrated the sensitisation of both Nd^{3+} and Yb^{3+} ions in aqueous environments with moderate NIR-emitting efficiency. The presence of a coordinated H_2O molecule (q = 0.9 and 1.0, respectively) – providing a non-radiative decay pathway – is partially to blame for the observed modest NIR quantum yields. Nevertheless, this synthetic scaffold may possess potential application in the conjugation of Ln^{3+}-based luminescent probes to various biomolecules.

Labelling amino acids and peptides enables the real-time monitoring of endogenous biological reactions and allows us to use low reagent concentrations. The practice of labelling peptides with conventional organic fluorophores is widespread in many biological assays, and is readily being expanded to harness the numerous benefits offered by luminescent lanthanide complexes. It is essential to exercise caution when choosing the coupling site and size of the lanthanide complex – to minimise any disruption to the enzymatic reaction. However, considering the extensive use of fluorescently labelled peptides, this is unlikely to pose a significant obstacle to the adoption of this technology. Anticipated progress in the development of lanthanide-based enzyme assays is on the horizon, offering potential attractive alternatives to current commercial assay formats, which may aid in the drug discovery process.

Peptide-probes with therapeutic and sensing capabilities

Peptide probes with dual therapeutic and sensing capabilities have the potential to address a critical need at the intersection of medicine and diagnostics. In the area of therapeutics, these probes offer a targeted approach for treating diseases. Simultaneously, the sensing capabilities of these peptide probes are invaluable for diagnostics and monitoring. By incorporating luminescent or other sensing properties, these probes can detect specific biomarkers indicative of diseases or physiological changes. This dual-functionality allows for real-time monitoring of treatment efficacy, enabling adjustments to therapeutic strategies based on the observed molecular responses.

In the context of personalised medicine, the combination of therapeutic and sensing capabilities in peptide probes provides a tailored and adaptable approach, allowing clinicians to optimise treatment-plans based on individual patient responses.[217] Overall, the integration of therapeutic and sensing capabilities in peptide probes addresses the growing demand for precision medicine, offering more effective and personalized treatments while advancing our ability to monitor and understand complex biological processes.

The group of J. S. Kim and colleagues have reported two fluorescent naphthalimide-based peptide theragnostic probes **Naph-1** and **Naph-2**, for the treatment of cancer (Fig. 26).[218,219]

Naph-1 utilised an RGD peptide sequence as its tumour-targeting motif, and employed camptothecin as its therapeutic agent – an anti-tumour inhibitor of topoisomerase I. This was also composed of a disulfide-linker coupled to a naphthalimide fluorophore, that produced a bathochromic fluorescence shift upon cleavage *via* glutathione or thioredoxin (species overexpressed in cancer cells). Indeed, the results indicated that Naph-1 was selectively up-taken by U87 tumour cells *via* a $\alpha_v\beta_3$ integrin-mediated mechanism, evidenced by competitive okadaic acid treatment. An "off–on" fluorescence change was observed (λ_{em} = 535 nm) upon reaction with glutathione, which released the camptothecin warhead into the nucleus of the cell. This could serve as an excellent theragnostic delivery platform, offering precise tumour targeting while allowing the monitoring of free drug concentration through changes in fluorescence signalling.

The group then employed a similar design strategy for the generation of Naph-2, which consisted of biotin (as the cancer targeting motif), a fluorescent naphthalimide reporter, and a Holliday Junction inhibitor peptide (KWWCRW) as the therapeutic. Like before, fragmentation occurred *via* disulfide-bond cleavage leading to the release of the inhibitor peptide, with the fluorescent signal being monitored in real-time. Although Kim *et al.* expertly showcase the application of the naphthalimide fluorophore in generating fluorogenic theragnostic prodrugs (Naph-1 & Naph-2), further research is needed to evaluate the translational potential of these compounds for clinical use, including pharmacokinetics, toxicity profiles, and efficacy in animal models.

In regard to lanthanide luminescence, Chau *et al.* synthesized DO3A-based Eu^{3+} and Yb^{3+} complexes, with appendaged P19 peptides (Pra-KAhx-K-LDLALK-FWLY-K-IVMSDKW-K-RrRK) designed to selectively bind to the latent-membrane protein I (LMP1) for visible and near-IR imaging and cancer monitoring (Epstein–Barr virus).[220]

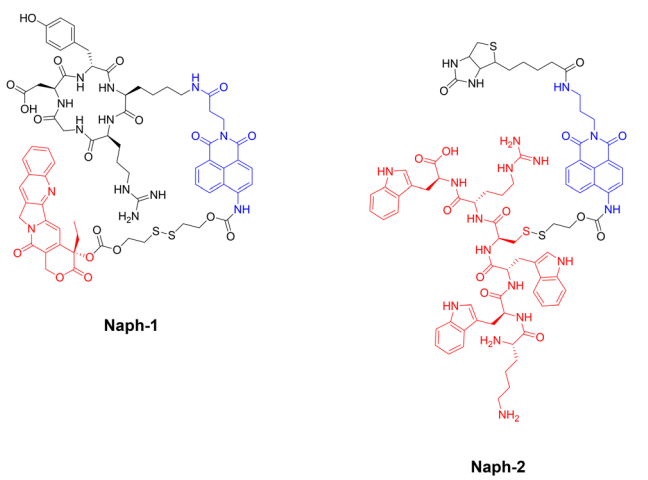

Fig. 26 Structures of fluorescent naphthalimide-based peptide theragnostic probes. Note: Sensing moiety highlighted in blue, and therapeutic agent in red.

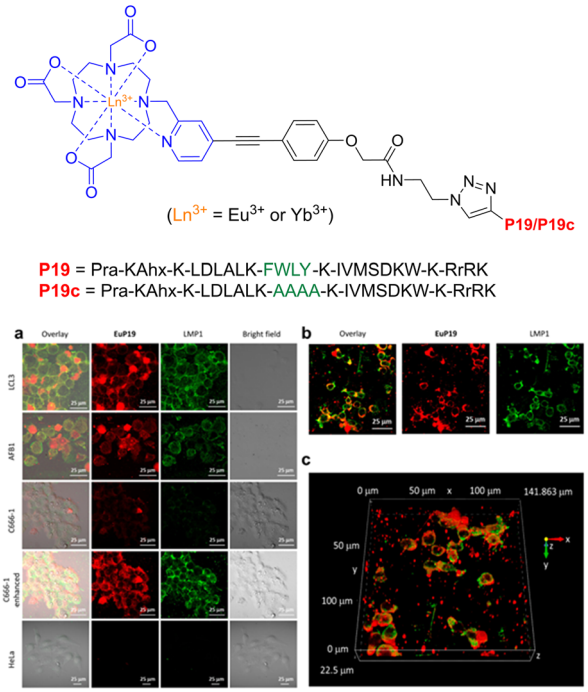

Fig. 27 Structure of lanthanide-based peptide probe, containing Eu^{3+} and Yb^{3+}. (a) Immunoluminescence imaging of the LMP1 protein and **EuP19** in LCL3, AFB1, C666-1, and HeLa cells after 12 h of incubation. (b) Immunoluminescence images of LMP1 and **EuP19** in LCL3 in the *xy* plane. (c) *Z*-Stacks of 2D images of LMP1 and **EuP19** in LCL3 cells (adapted from ref. 220 with permission from American Chemical Society, copyright 2021).[220]

Due to the pivotal role of the FWLY sequence in regulating the signalling pathway, peptide P19 was synthesized to emulate the essential amino acid residues found in the transmembrane region of LMP1. Propargyl-glycine (Pra) was introduced into the peptide-backbone to facilitate conjugation between P19 and the Ln^{3+} complex *via* click chemistry.

The subcellular localisation of LMP1 expression was then investigated by immunoluminescence imaging (Fig. 27). Overlapping of the LMP1 (green) signal with the EuP19 (red) signal was observed in LCL3 and AFB1 cells after 12 hours, with EuP19 colocalising with LMP1 in the LCL3 cell-membrane – highlighted by the overlayed yellow signals. Similar images were recorded for EuP19 in C666-1 cells, but with dramatically decreased luminescence intensity. No luminescent signal was observed for both EuP19 and LMP1 in LMP1-negative HeLa cells, suggesting that EuP19 is selective for cells that express LMP1. Although the emission quantum yield of EuP19 was 8.3 (±0.8%), YbP19 was relatively low at 0.05 (±0.005%), indicating room for improvement in terms of enhancing the efficiency of the NIR emission. Be that as it may, this study discloses a novel method for live-visualisation of LMP1 in Epstein–Barr virus tumour cells, with subsequent selective cytotoxicity for LMP1-positive cells by suppressing the NF-$_K$B pathway.

This theragnostic approach may have clinical importance as tumours expressing LMP1 are recognised for their heightened aggressiveness compared to LMP1-negative tumours, making them more susceptible to lymph node metastasis.[221] Additionally, LMP1-positive tumours are linked to poorer overall survival, with LMP1 serving as a robust risk factor for unfavourable prognosis in patients with nasopharyngeal cancer.[222]

Other fluorescent/luminescent anti-cancer peptide probes have been reported for targeting discrete proteins.[223,224] However, these larger supramolecular structures will be discussed in more detail in the next section. Thus, we limit the current selection to small-molecule theragnostic peptide probes.

Peptide-modulated self-assembly of luminescent structures

The L-Phe-L-Phe (FF) dipeptide motif represents the most basic sequence displaying self-assembling traits. The self-assembly of FF draws inspiration from the development of amyloid plaques formed by polypeptides – containing FF – during the progression of Alzheimer's disease.[225] The FF dipeptide has proven to be a versatile building-block for the supramolecular construction of well-organized nanostructures.[226,227] FF self-assemblies can also evoke different morphologies,[228] induce controlled patterning,[229] and facilitate dimensional control over assembled nanostructures.[230] In contrast to other self-assembling peptides, aromatic dipeptides offer the advantages of synthetic versatility, small molecular structure(s), and reduced experimental costs. These attributes are highly valuable for both elucidating inherent self-assembly mechanisms and tailoring properties for specific applications. Indeed, Q. Zou[231] and K. Tao[232] (amongst others) have produced fantastic review articles documenting many of these applications, and have provided in-depth explanations for

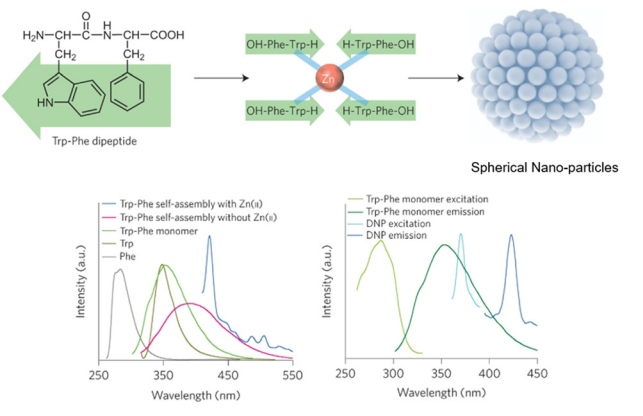

Fig. 28 Design strategy for fluorescent nanoparticles *via* L-Trp-L-Phe self-assembly. (Bottom left) Various fluorescent emission spectra. (Bottom right) Fluorescent excitation and emission spectra of dipeptide monomers *vs.* self-assembled nanoparticles.[235]

this ubiquitous self-assembly phenomenon. We highly recommend reading their work for a more detailed account of peptide-based supramolecular chemistry. With that said, this section will solely focus on select examples of peptide-modulated self-assembly of luminescent supramolecular structures.

Self-assembled peptide nanostructures have been used in the construction of biological and biomedical applications, leveraging their unique attributes such as biocompatibility and tuneable self-assembly.[233] In drug delivery, these nanostructures serve as targeted carriers, enabling controlled release with minimal side-effects. They play a vital role in imaging and diagnosis, acting as contrast agents and biosensors for various modalities.[234]

The Zhang group demonstrated the self-assembly of L-Trp-L-Phe nanoparticles that shifted the native peptide's fluorescent output from the UV- to the visible-region.[235] The essence of their design strategy was inspired by two natural phenomena; the molecular mechanism responsible for the red-shift in the yellow fluorescent protein (YFP) and the enhanced fluorescence intensity observed in the green fluorescent mutant protein BFPms1. The bathochromic shift in YFP is a direct result of π–π stacking,[236] with the fluorescent enhancement of BFPms1 arising from the structural rigidification by Zn(II).[237] Following the reaction of the (L-Trp-L-Phe) dipeptides with $ZnCl_2$ (dissolved in a mixture of methanol and aq. sodium hydroxide), atomic force microscopy (AFM) and transmission electron microscopy (TEM) revealed the formation of uniform spherical nanoparticles (Fig. 28).

The photophysical properties of the nanoparticles were then investigated. The Zn^{2+}-chelated (L-Trp-L-Phe) nanoparticles possessed a fluorescence emission maxima at 423 nm, which was red-shifted 33 nm compared to the dipeptide assemblies without Zn^{2+} coordination (390 nm). Fluorescence microscopy images of the Zn-bound nanoparticles were recorded, with bright-blue fluorescence being observed. The group then went on to compare the photostability and biocompatibility of the novel peptide nanoparticles against a fluorescent rhodamine dye (Rh6G) and CdSe quantum dots in NIH-3T3 cells, respectively. After continuous irradiation, the nanoparticles remained stable, indicating enhanced photostability compared to the Rh6G dye. The MTT assay suggested that the nanoparticles were far more biocompatible than the CdSe quantum dots.

A theragnostic approach utilising these L-Trp-L-Phe nanoparticles was then explored for the potential visualisation of drug-release in real-time. Doxorubicin (DOX) has been shown to adsorb onto nanoparticles with appropriate functionalities,[238] with π–π stacking and N–H–π electrostatic forces dominating this attractive interaction.[239] The interaction between DOX and the nanoparticles was characterised by their fluorescent and absorbance spectra, with the authors claiming that the reduced absorbance at 480 nm and fluorescent quenching at 595 nm pertained to the electrostatic interactions between the nanoparticles and DOX. This was further investigated with fluorescent imaging in A549 cells. Minimal red fluorescence was observed from the cells incubated with DOX/nanoparticle-conjugates, compared to cells treated with only DOX. This indicated that fluorescent-quenching was likely due to contact with the L-Trp-L-Phe nanoparticles (Fig. 29).

After an extended period of incubation (12 hours), more DOX was gradually released, leading to an increase in fluorescence signal for both free DOX and nanoparticle. These results indicate that this DOX/Trp-Phe nanoparticle-conjugate design strategy may have promising potential to act as a peptide–drug nanostructure for the visualisation of DOX release in real-time. In comparison to organic fluorophores – which are usually perturbed by photo-bleaching and broad emission bands – and quantum dots

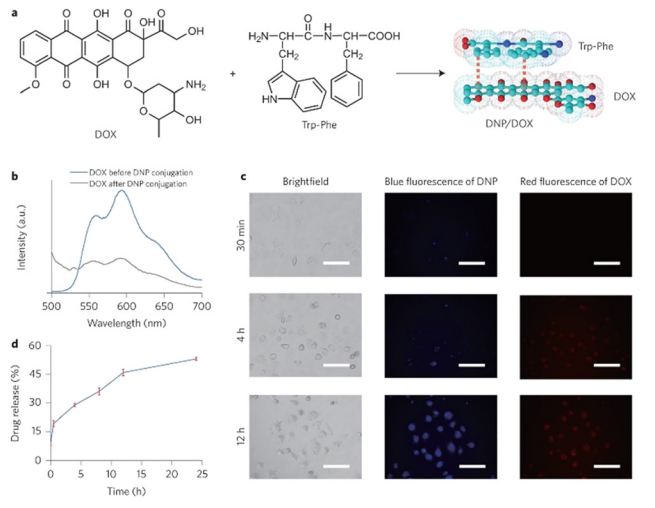

Fig. 29 (a) DOX coordinated to the L-Trp-L-Phe nanoparticles *via* π–π stacking. (b) Fluorescence emission spectra of DOX before and after nanoparticle-coordination. (c) Fluorescence imaging of the DOX/nanoparticle-conjugates in A549 cells over time. (d) Time-dependent drug-release of DOX from the DOX/nanoparticle-conjugates.[235]

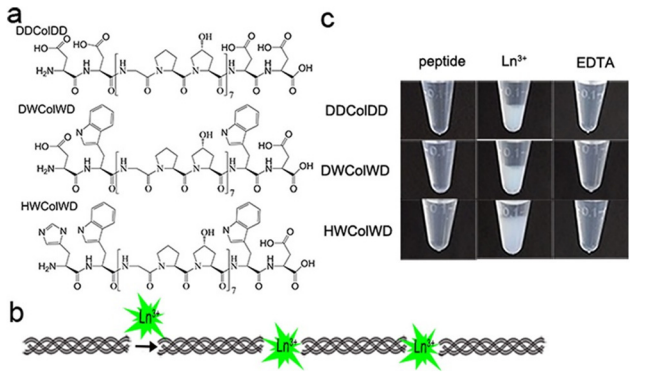

Fig. 30 Ln^{3+}-triggered assembly of collagen-mimetic peptides. (a) Amino-acid sequences of three collagen-mimetic peptides. (b) Schematic illustration of the self-assembly reaction. (c) Changes of the peptide-solution with, and without Ln^{3+} ions/EDTA (reprinted from ref. 241 with permission from American Chemical Society, copyright 2019).[241]

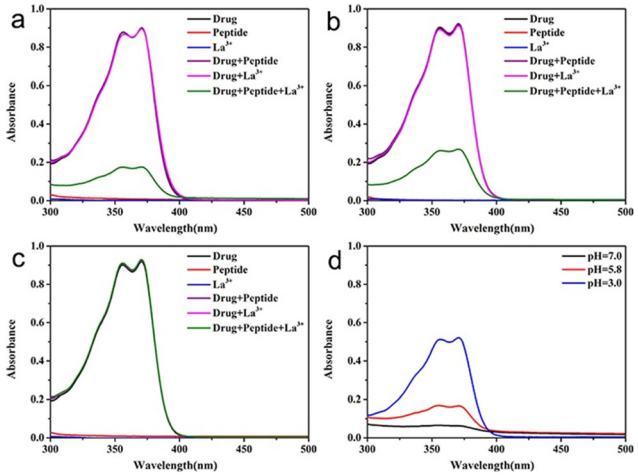

Fig. 31 Drug-loading and release of camptothecin *via* DDColDD–La^{3+}. Absorbance spectra at (a) pH = 7.0, (b) pH = 5.8, (c) pH = 3.0. Absorbance spectra of camptothecin release within the supernatant after 24 h (d) (reprinted from ref. 241 with permission from American Chemical Society, copyright 2019).[241]

(solubility and biocompatibility concerns),[240] Zhang and coworkers have demonstrated that their (L-Trp-L-Phe) nanoparticles are biocompatible, photostable and possess visible fluorescent characteristics.

Another interesting example of self-assembled peptide supramolecular structures comes from the group of Xiao and colleagues, in which they report the synthesis of luminescent lanthanide–collagen peptide-hybrid nanofibers, for pH-controlled drug delivery.[241] This strategy takes inspiration from the biomimetic-scaffold – which has been often employed in tissue-engineering and regenerative medicine.[242,243]

The synthesized collagen peptides all contained a Gly-Pro-Hyp (GPO) repeating unit, which is understood to be one of the most-stabilising sequences for triple-helix structures.[244] Aspartic acid residues were then functionalised at each peptide-terminus to form the coordination sphere around the Ln^{3+} ions and between the collagen-mimetic peptides. The initial synthesized peptide (DDColDD) contained an Asp-Asp dipeptide at each terminus for Ln^{3+} coordination. The design strategy behind the next synthetic peptide (DWColWD) was two-fold; replacement of D-residues with W-residues to probe how the composition of amino acids at each terminus affects the self-assembly, and W-residues can be used an antenna for Ln^{3+} luminescence.[245] A third and final synthetic peptide was constructed (HWColWD) by replacing the N-terminal D-residue with a H-residue as an additional coordination-site for the Ln^{3+} ions (Fig. 30).

Various Ln^{3+} ions (Tb^{3+}, Ce^{3+}, Eu^{3+}, La^{3+}, Tm^{3+}, Er^{3+} and Yb^{3+}) were mixed with the DDColDD, DWColWD and HWColWD peptides to investigate their self-assembly. Fig. 30 demonstrated that all the Ln^{3+} ions caused the peptide solutions to become turbid, suggesting lanthanide-induced self-assembly. The reversibility of this assembly was also highlighted by the clear solution upon addition of EDTA, which effectively sequestered the Ln^{3+} ions.

The pH-responsive characteristics of the collagen-mimetic peptide–lanthanide structures were explored for their potential application as drug-carriers. Camptothecin, a commonly employed substance for evaluating the delivery efficiency of anticancer drugs,[246] served as a model drug in this investigation (Fig. 31).

The peptide chosen for this study was DDColDD. Mixtures of peptide DDColDD and camptothecin were generated at pH 7.0, 5.8, and 3.0. Upon the addition of La^{3+} ions to the mixtures at pH = 7.0 and pH = 5.8, aggregates were promptly formed, enveloping the camptothecin. The supernatant – obtained by removing the aggregates – was then collected, and the camptothecin content was determined using UV-analysis, with the highest camptothecin-loading value being observed at pH 7.0. Complementary camptothecin-release studies were then conducted for the same peptide under the same pH conditions (7.0, 5.8 & 3.0). The drug-release results were as follows: pH 3.0 > 5.8 > 7.0, with the highest amount being released at pH = 3.0 (34.3 mg g^{-1}). Cefoperazone sodium – a popular antibiotic[247,248] – was also investigated as an example drug-model. The absorbance spectra of the solution containing cefoperazone alongside the synthetic peptide or La^{3+} ions (or both) closely resembled the absorbance profile of the free-drug. This similarity suggested that these species would not interfere in the absorbance measurements of cefoperazone. When subject to the same pH-mediated drug-loading and release experiments, maximum loading was achieved a pH = 7.0, with the largest drug-release being observed at pH = 3.0 (111.3 mg g^{-1}). These findings suggest that a diverse range of drugs can be effectively loaded using the collagen peptide–lanthanide scaffolds.

The self-assembly of all three collagen-peptides (DDColDD, DWColWD, and HWColWD) facilitated by Ln^{3+} ions has been successfully demonstrated, and found to be reversibly controlled by pH. The pH-dependent variations of these assemblies can be modulated by the specific functionality of the terminal amino acids. Employing camptothecin and cefoperazone as example drugs, the loading and releasing efficiency of the collagen peptide–lanthanide scaffolds were also examined. While the *in vitro* results are promising, future studies could focus on *in vivo* experiments to evaluate the efficacy and safety of the luminescent lanthanide–collagen peptide scaffolds for drug delivery in living systems, considering factors like tissue distribution, metabolism, and long-term effects.

There are many other interesting and noteworthy studies that have been documented regarding peptide-probes as luminescent supramolecular sensors.[249–252] However, this brief perspective was not intended to be an exhaustive report, more a succinct portrayal of the extensive applications available to synthetically modified peptides.

Conclusions

The evolution of chemical methods for peptide synthesis has not only expanded our capabilities for generating complex peptide structures but has also paved the way for innovative applications in various scientific domains. The strategic chemical modification of peptides has improved their overall performance and biocompatibility, enabling their integration into diverse research and therapeutic endeavours.

Moreover, the emergence of fluorescent and luminescent peptide conjugates has brought a new dimension to the field, with these conjugates serving as valuable tools for creating highly sensitive and specific sensing technologies. As peptides continue to play an indispensable role in uniting the realms of chemistry and biology, their potential for future discoveries and applications remains boundless. This brief perspective, from the therapeutic history of peptides to their luminescent application in supramolecular scaffolds, underscores their enduring significance in shaping the interdisciplinary landscape of modern chemistry and sets the stage for exciting progress in the years to come.

Conflicts of interest

There are no conflicts to declare.

Acknowledgements

The authors would like to acknowledge funding from Science Foundation Ireland (SFI), grant number 12/RC/2275/P2, which is co-funded under the European Regional Development Fund. This article is based upon discussions emanting from COST Action CA22131 Supramolecular LUminescent Chemosensors for Environmental Security (LUCES), supported by COST (European Cooperation in Science and Technology).

References

1 R. H. A. Plimmer, *The Chemical Constitution of the Proteins Part II*, Read Books, 2008.
2 D. A. Scott and C. H. Best, *Ind. Eng. Chem.*, 1925, **17**, 238–240.
3 M. Bliss, F. G. Banting, C. H. Best and J. B. Collip, *Bull. Hist. Med.*, 1982, **56**, 554–568.
4 V. du Vigneaud, C. Ressler, J. M. Swan, C. W. Roberts and P. G. Katsoyannis, *J. Am. Chem. Soc.*, 1954, **76**, 3115–3121.
5 B. Merrifield, *Science*, 1986, **232**, 341–347.
6 M. Muttenthaler, G. F. King, D. J. Adams and P. F. Alewood, *Nat. Rev. Drug Discovery*, 2021, **20**, 309–325.
7 D. F. Steiner, in *Encyclopedia of Endocrine Diseases*, ed. L. Martini, Elsevier, New York, 2004, pp. 545–555.
8 M. A. Gonzalez-Lozano and K. W. Li, in *eLS*, 2020, pp. 1–9.
9 A. U. Dignass and A. Sturm, *Eur. J. Gastroenterol. Hepatol.*, 2001, **13**, 763–770.
10 J. L. Lau and M. K. Dunn, *Bioorg. Med. Chem.*, 2018, **26**, 2700–2707.
11 A. Muheem, F. Shakeel, M. A. Jahangir, M. Anwar, N. Mallick, G. K. Jain, M. H. Warsi and F. J. Ahmad, *Saudi Pharm. J.*, 2016, **24**, 413–428.
12 A. T. Zizzari, D. Pliatsika, F. M. Gall, T. Fischer and R. Riedl, *Drug Discovery Today*, 2021, **26**, 1097–1105.
13 S. S. Usmani, G. Bedi, J. S. Samuel, S. Singh, S. Kalra, P. Kumar, A. A. Ahuja, M. Sharma, A. Gautam and G. P. S. Raghava, *PLoS One*, 2017, **12**, e0181748.
14 T. M. Research, Peptide Therapeutics Market Outlook 2031, **https://www.transparencymarketresearch.com/peptide-therapeutics-market.html**, (accessed October, 2022).
15 J. N. Shah, G.-Q. Guo, A. Krishnan, M. Ramesh, N. K. Katari, M. Shahbaaz, M. H. Abdellattif, S. K. Singh and K. Dua, *Therapies*, 2022, **77**, 319–328.
16 J. H. Park, J. H. Moon, H. J. Kim, M. H. Kong and Y. H. Oh, *Korean J. Fam. Med.*, 2020, **41**, 365–373.
17 K. Imai and A. Takaoka, *Nat. Rev. Cancer*, 2006, **6**, 714–727.
18 K. Fosgerau and T. Hoffmann, *Drug Discovery Today*, 2015, **20**, 122–128.
19 J. Davda, P. Declerck, S. Hu-Lieskovan, T. P. Hickling, I. A. Jacobs, J. Chou, S. Salek-Ardakani and E. Kraynov, *J. Immunother. Cancer*, 2019, **7**, 105.
20 A. J. Smith, *SLAS Discovery*, 2015, **20**, 437–453.
21 L. Diao and B. Meibohm, *Clin. Pharmacokinet.*, 2013, **52**, 855–868.
22 L. Wang, N. Wang, W. Zhang, X. Cheng, Z. Yan, G. Shao, X. Wang, R. Wang and C. Fu, *Signal Transduction Targeted Ther.*, 2022, **7**, 48.
23 P. W. J. M. Frederix, G. G. Scott, Y. M. Abul-Haija, D. Kalafatovic, C. G. Pappas, N. Javid, N. T. Hunt, R. V. Ulijn and T. Tuttle, *Nat. Chem.*, 2015, **7**, 30–37.
24 J. Zhou, X. Du, N. Yamagata and B. Xu, *J. Am. Chem. Soc.*, 2016, **138**, 3813–3823.
25 T. A. Martinek, A. Hetényi, L. Fülöp, I. M. Mándity, G. K. Tóth, I. Dékány and F. Fülöp, *Angew. Chem., Int. Ed.*, 2006, **45**, 2396–2400.
26 H. Cui, M. J. Webber and S. I. Stupp, *Pept. Sci.*, 2010, **94**, 1–18.
27 E. Gazit, *Chem. Soc. Rev.*, 2007, **36**, 1263–1269.
28 X. Yan, J. Li and H. Möhwald, *Adv. Mater.*, 2011, **23**, 2796–2801.
29 J. B. Matson and S. I. Stupp, *Chem. Commun.*, 2012, **48**, 26–33.
30 S. Chandrudu, P. Simerska and I. Toth, *Molecules*, 2013, **18**, 4373–4388.
31 G. W. Anderson and A. C. McGregor, *J. Am. Chem. Soc.*, 1957, **79**, 6180–6183.
32 D. S. Kemp, S.-L. Leung and D. J. Kerkman, *Tetrahedron Lett.*, 1981, **22**, 181–184.
33 P. E. Dawson, T. W. Muir, I. Clark-Lewis and S. B. H. Kent, *Science*, 1994, **266**, 776–779.
34 T. W. Muir, D. Sondhi and P. A. Cole, *Proc. Natl. Acad. Sci. U. S. A.*, 1998, **95**, 6705–6710.
35 B. L. Nilsson, L. L. Kiessling and R. T. Raines, *Org. Lett.*, 2000, **2**, 1939–1941.

36 M. Skwarczynski and Y. Kiso, *Curr. Med. Chem.*, 2007, **14**, 2813–2823.
37 L. Di, *AAPS J.*, 2015, **17**, 134–143.
38 A. Schaller, in *Studies in Natural Products Chemistry*, ed. R. Atta ur, Elsevier, 2001, vol. 25, pp. 367–411.
39 B. S. Davidson, *Chem. Rev.*, 1993, **93**, 1771–1791.
40 N. Fusetani and S. Matsunaga, *Chem. Rev.*, 1993, **93**, 1793–1806.
41 Y. Hamada and T. Shioiri, *Chem. Rev.*, 2005, **105**, 4441–4482.
42 U. Kazmaier and J. Deska, *Curr. Org. Chem.*, 2008, **12**, 355–385.
43 M. Pelay-Gimeno, A. Glas, O. Koch and T. N. Grossmann, *Angew. Chem., Int. Ed.*, 2015, **54**, 8896–8927.
44 E. Lenci and A. Trabocchi, *Chem. Soc. Rev.*, 2020, **49**, 3262–3277.
45 M. Pasco, C. Dolain and G. Guichard, in *Comprehensive Supramolecular Chemistry II*, ed. J. L. Atwood, Elsevier, Oxford, 2017, pp. 89–125.
46 A. Henninot, J. C. Collins and J. M. Nuss, *J. Med. Chem.*, 2018, **61**, 1382–1414.
47 E. Masri, Ahsanullah, M. Accorsi and J. Rademann, *Org. Lett.*, 2020, **22**, 2976–2980.
48 K. Wiśniewski, R. Galyean, H. Tariga, S. Alagarsamy, G. Croston, J. Heitzmann, A. Kohan, H. Wiśniewska, R. Laporte, P. J. M. Rivière and C. D. Schteingart, *J. Med. Chem.*, 2011, **54**, 4388–4398.
49 A. F. M. Noisier and M. A. Brimble, *Chem. Rev.*, 2014, **114**, 8775–8806.
50 W. Gong, G. Zhang, T. Liu, R. Giri and J.-Q. Yu, *J. Am. Chem. Soc.*, 2014, **136**, 16940–16946.
51 B. V. Popp and Z. T. Ball, *Chem. Sci.*, 2011, **2**, 690–695.
52 N. Brot and H. Weissbach, *Trends Biochem. Sci.*, 1982, **7**, 137–139.
53 J. B. Jones and D. W. Hysert, *Can. J. Chem.*, 1971, **49**, 3012–3019.
54 V. Frey, J. Viaud, G. Subra, N. Cauquil, J.-F. Guichou, P. Casara, G. Grassy and A. Chavanieu, *Eur. J. Med. Chem.*, 2008, **43**, 966–972.
55 C. Haskell-Luevano, K. Toth, L. Boteju, C. Job, A. M. D. L. Castrucci, M. E. Hadley and V. J. Hruby, *J. Med. Chem.*, 1997, **40**, 2740–2749.
56 H. Ban, J. Gavrilyuk and C. F. Barbas, III, *J. Am. Chem. Soc.*, 2010, **132**, 1523–1525.
57 H. Ban, M. Nagano, J. Gavrilyuk, W. Hakamata, T. Inokuma and C. F. Barbas, III, *Bioconjugate Chem.*, 2013, **24**, 520–532.
58 Z. Ruan, N. Sauermann, E. Manoni and L. Ackermann, *Angew. Chem., Int. Ed.*, 2017, **56**, 3172–3176.
59 M. B. Hansen, F. Hubálek, T. Skrydstrup and T. Hoeg-Jensen, *Chem. – Eur. J.*, 2016, **22**, 1572–1576.
60 J. M. Chalker, G. J. L. Bernardes, Y. A. Lin and B. G. Davis, *Chem. – Asian J.*, 2009, **4**, 630–640.
61 B. Bernardim, P. M. S. D. Cal, M. J. Matos, B. L. Oliveira, N. Martínez-Sáez, I. S. Albuquerque, E. Perkins, F. Corzana, A. C. B. Burtoloso, G. Jiménez-Osés and G. J. L. Bernardes, *Nat. Commun.*, 2016, **7**, 13128.
62 A. Abbas, B. Xing and T.-P. Loh, *Angew. Chem., Int. Ed.*, 2014, **53**, 7491–7494.
63 E. V. Vinogradova, C. Zhang, A. M. Spokoyny, B. L. Pentelute and S. L. Buchwald, *Nature*, 2015, **526**, 687–691.
64 J. Chatterjee, F. Rechenmacher and H. Kessler, *Angew. Chem., Int. Ed.*, 2013, **52**, 254–269.
65 R. W. Cheloha, T. Watanabe, T. Dean, S. H. Gellman and T. J. Gardella, *ACS Chem. Biol.*, 2016, **11**, 2752–2762.
66 J. A. Schneider, T. W. Craven, A. C. Kasper, C. Yun, M. Haugbro, E. M. Briggs, V. Svetlov, E. Nudler, H. Knaut, R. Bonneau, M. J. Garabedian, K. Kirshenbaum and S. K. Logan, *Nat. Commun.*, 2018, **9**, 4396.
67 X. Wei, C. Zhan, X. Chen, J. Hou, C. Xie and W. Lu, *Mol. Pharmaceutics*, 2014, **11**, 3261–3268.
68 R. Laporte, A. Kohan, J. Heitzmann, H. Wiśniewska, J. Toy, E. La, H. Tariga, S. Alagarsamy, B. Ly, J. Dykert, S. Qi, K. Wiśniewski, R. Galyean, G. Croston, C. D. Schteingart and P. J. M. Rivière, *J. Pharmacol. Exp. Ther.*, 2011, **337**, 786.
69 P.-F. Laterre, S. M. Berry, A. Blemings, J. E. Carlsen, B. François, T. Graves, K. Jacobsen, R. J. Lewis, S. M. Opal, A. Perner, P. Pickkers, J. A. Russell, N. A. Windeløv, D. M. Yealy, P. Asfar, M. H. Bestle, G. Muller, C. Bruel, N. Brulé, J. Decruyenaere, A.-M. Dive, T. Dugernier, K. Krell, J.-Y. Lefrant, B. Megarbane, E. Mercier, J.-P. Mira, J.-P. Quenot, B. S. Rasmussen, H.-C. Thorsen-Meyer, M. Vander Laenen, M. L. Vang, P. Vignon, I. Vinatier, S. Wichmann, X. Wittebole, A. L. Kjølbye, D. C. Angus and for the SEPSIS-ACT Investigators, *JAMA, J. Am. Med. Assoc.*, 2019, **322**, 1476–1485.
70 H. G. Bossler and D. Seebach, *Helv. Chim. Acta*, 1994, **77**, 1124–1165.
71 D. Seebach, A. K. Beck, H. G. Bossler, C. Gerber, S. Y. Ko, C. W. Murtiashaw, R. Naef, S.-I. Shoda, A. Thaler, M. Krieger and R. Wenger, *Helv. Chim. Acta*, 1993, **76**, 1564–1590.
72 S. Datta, A. Bayer and U. Kazmaier, *Org. Biomol. Chem.*, 2012, **10**, 8268–8275.
73 L. Zhao, O. Baslé and C.-J. Li, *Proc. Natl. Acad. Sci. U. S. A.*, 2009, **106**, 4106–4111.
74 T. J. Osberger, D. C. Rogness, J. T. Kohrt, A. F. Stepan and M. C. White, *Nature*, 2016, **537**, 214–219.
75 C. J. White and A. K. Yudin, *Nat. Chem.*, 2011, **3**, 509–524.
76 C. Heinis, *Nat. Chem. Biol.*, 2014, **10**, 696–698.
77 D. F. Veber, R. M. Freidinger, D. S. Perlow, W. J. Paleveda, F. W. Holly, R. G. Strachan, R. F. Nutt, B. H. Arison, C. Homnick, W. C. Randall, M. S. Glitzer, R. Saperstein and R. Hirschmann, *Nature*, 1981, **292**, 55–58.
78 H. Kessler, *Angew. Chem., Int. Ed. Engl.*, 1982, **21**, 512–523.
79 C. K. Wang and D. J. Craik, *Nat. Chem. Biol.*, 2018, **14**, 417–427.
80 M. L. J. Korsinczky, H. J. Schirra, K. J. Rosengren, J. West, B. A. Condie, L. Otvos, M. A. Anderson and D. J. Craik, *J. Mol. Biol.*, 2001, **311**, 579–591.
81 M. L. Colgrave, M. J. L. Korsinczky, R. J. Clark, F. Foley and D. J. Craik, *Pept. Sci.*, 2010, **94**, 665–672.
82 A. Parenty, X. Moreau and J. M. Campagne, *Chem. Rev.*, 2006, **106**, 911–939.

83 C. A. G. N. Montalbetti and V. Falque, *Tetrahedron*, 2005, **61**, 10827–10852.
84 F. Albericio, R. P. Hammer, C. GarcÍA-EcheverrÍA, M. A. Molins, J. L. Chang, M. C. Munson, M. Pons, E. Giralt and G. Barany, *Int. J. Pept. Protein Res.*, 1991, **37**, 402–413.
85 C. F. McCusker, P. J. Kocienski, F. T. Boyle and A. G. Schätzlein, *Bioorg. Med. Chem. Lett.*, 2002, **12**, 547–549.
86 S. A. Kates, N. A. Solé, C. R. Johnson, D. Hudson, G. Barany and F. Albericio, *Tetrahedron Lett.*, 1993, **34**, 1549–1552.
87 C. Bechtler and C. Lamers, *RSC Med. Chem.*, 2021, **12**, 1325–1351.
88 H. B. B:urgi, J. D. Dunitz, J. M. Lehn and G. Wipff, *Tetrahedron*, 1974, **30**, 1563–1572.
89 V. Martí-Centelles, M. D. Pandey, M. I. Burguete and S. V. Luis, *Chem. Rev.*, 2015, **115**, 8736–8834.
90 U. Schmidt and J. Langner, *J. Pept. Res.*, 1997, **49**, 67–73.
91 P. M. Hardy, G. W. Kenner and R. C. Sheppard, *Tetrahedron*, 1963, **19**, 95–105.
92 R. W. Hoffmann, *Angew. Chem., Int. Ed. Engl.*, 1992, **31**, 1124–1134.
93 I. Daidone, H. Neuweiler, S. Doose, M. Sauer and J. C. Smith, *PLoS Comput. Biol.*, 2010, **6**, e1000645.
94 J. A. Smith, L. G. Pease and K. D. Kopple, *Crit. Rev. Biochem.*, 1980, **8**, 315–399.
95 M. Rothe, K. D. Steffen and I. Rothe, *Angew. Chem., Int. Ed. Engl.*, 1965, **4**, 356–356.
96 M. Favre, K. Moehle, L. Jiang, B. Pfeiffer and J. A. Robinson, *J. Am. Chem. Soc.*, 1999, **121**, 2679–2685.
97 Y. Takeuchi and G. R. Marshall, *J. Am. Chem. Soc.*, 1998, **120**, 5363–5372.
98 H. Kessler and B. Haase, *Int. J. Pept. Protein Res.*, 1992, **39**, 36–40.
99 M. Tamaki, S. Akabori and I. Muramatsu, *J. Am. Chem. Soc.*, 1993, **115**, 10492–10496.
100 M. Liu, Y. C. Tang, K. Q. Fan, X. Jiang, L. H. Lai and Y. H. Ye, *J. Pept. Res.*, 2005, **65**, 55–64.
101 J. Wu, J. Tang, H. Chen, Y. He, H. Wang and H. Yao, *Tetrahedron Lett.*, 2018, **59**, 325–333.
102 M. R. Eshelman, A. R. Aldous, K. P. Neupane and J. A. Kritzer, *Tetrahedron*, 2014, **70**, 7651–7654.
103 A. Kotynia, J. S. Pap and J. Brasun, *Inorg. Chim. Acta*, 2018, **472**, 3–11.
104 K. Haas, W. Ponikwar, H. Nöth and W. Beck, *Angew. Chem., Int. Ed.*, 1998, **37**, 1086–1089.
105 I. Alfonso, M. Bolte, M. Bru, M. I. Burguete, S. V. Luis and J. Rubio, *J. Am. Chem. Soc.*, 2008, **130**, 6137–6144.
106 V. Martí-Centelles, M. I. Burguete and S. V. Luis, *J. Org. Chem.*, 2016, **81**, 2143–2147.
107 N. Vidović, G. Horvat, D. Riva, T. Rinkovec, N. Cindro, V. Tomišić and G. Speranza, *Org. Lett.*, 2020, **22**, 2129–2134.
108 R. B. P. Elmes and K. A. Jolliffe, *Chem. Commun.*, 2015, **51**, 4951–4968.
109 P. G. Young, J. K. Clegg, M. Bhadbhade and K. A. Jolliffe, *Chem. Commun.*, 2011, **47**, 463–465.
110 E. Fischer, *Ber. Dtsch. Chem. Ges.*, 1891, **24**, 2683–2687.
111 H. A. Krebs, *Biochem. J.*, 1935, **29**, 1620–1644.
112 M. Seia and E. Zisman, *FASEB J.*, 1997, **11**, 449–456.
113 R. Tugyi, K. Uray, D. Iván, E. Fellinger, A. Perkins and F. Hudecz, *Proc. Natl. Acad. Sci. U. S. A.*, 2005, **102**, 413–418.
114 H. M. Werner, C. C. Cabalteja and W. S. Horne, *ChemBioChem*, 2016, **17**, 712–718.
115 S.-i. Wada, H. Tsuda, T. Okada and H. Urata, *Bioorg. Med. Chem. Lett.*, 2011, **21**, 5688–5691.
116 P. Ehrlich, in *The Collected Papers of Paul Ehrlich*, ed. F. Himmelweit, Pergamon, 2013, pp. 596–618.
117 G. Mathé, T. B. Loc and J. Bernard, *C. R. Hebd. Seances Acad. Sci.*, 1958, **246**, 1626–1628.
118 T. Ghose, M. Cerini, M. Carter and R. C. Nairn, *Br. Med. J.*, 1967, **1**, 90.
119 C. H. Ford, C. E. Newman, J. R. Johnson, C. S. Woodhouse, T. A. Reeder, G. F. Rowland and R. G. Simmonds, *Br. J. Cancer*, 1983, **47**, 35–42.
120 P. F. Bross, G. Beitz, X. H. Chen, E. Chen, L. Duffy, S. Kieffer, R. Roy, A. Sridhara, G. Rahman, R. Williams and R. Pazdur, *Clin. Cancer Res.*, 2001, **7**, 1490–1496.
121 A. A. Kaspar and J. M. Reichert, *Drug Discovery Today*, 2013, **18**, 807–817.
122 X. Sun, J. F. Ponte, N. C. Yoder, R. Laleau, J. Coccia, L. Lanieri, Q. Qiu, R. Wu, E. Hong, M. Bogalhas, L. Wang, L. Dong, Y. Setiady, E. K. Maloney, O. Ab, X. Zhang, J. Pinkas, T. A. Keating, R. Chari, H. K. Erickson and J. M. Lambert, *Bioconjugate Chem.*, 2017, **28**, 1371–1381.
123 M. Alas, A. Saghaeidehkordi and K. Kaur, *J. Med. Chem.*, 2021, **64**, 216–232.
124 T. L. Huang, A. Székács, T. Uematsu, E. Kuwano, A. Parkinson and B. D. Hammock, *Pharm. Res.*, 1993, **10**, 639–648.
125 H. Shi, R. T. K. Kwok, J. Liu, B. Xing, B. Z. Tang and B. Liu, *J. Am. Chem. Soc.*, 2012, **134**, 17972–17981.
126 G. M. Dubowchik, R. A. Firestone, L. Padilla, D. Willner, S. J. Hofstead, K. Mosure, J. O. Knipe, S. J. Lasch and P. A. Trail, *Bioconjugate Chem.*, 2002, **13**, 855–869.
127 A. Régina, M. Demeule, C. Ché, I. Lavallée, J. Poirier, R. Gabathuler, R. Béliveau and J. P. Castaigne, *Br. J. Pharmacol.*, 2008, **155**, 185–197.
128 D. L. Bushnell and K. L. Bodeker, *Hematol./Oncol. Clin. North Am.*, 2020, **29**, 317–326.
129 O. Rogoza, K. Megnis, M. Kudrjavceva, A. Gerina-Berzina and V. Rovite, *Int. J. Mol. Sci.*, 2022, **23**, 1447.
130 S. Banerjee, M. R. A. Pillai and F. F. Knapp, *Chem. Rev.*, 2015, **115**, 2934–2974.
131 F. Vacondio, C. Silva, M. Mor and B. Testa, *Drug Metab. Rev.*, 2010, **42**, 551–589.
132 S. K. Kumar, S. A. Williams, J. T. Isaacs, S. R. Denmeade and S. R. Khan, *Bioorg. Med. Chem.*, 2007, **15**, 4973–4984.
133 A. K. Ghosh and M. Brindisi, *J. Med. Chem.*, 2015, **58**, 2895–2940.
134 Y. Liang, S. Li, X. Wang, Y. Zhang, Y. Sun, Y. Wang, X. Wang, B. He, W. Dai, H. Zhang, X. Wang and Q. Zhang, *J. Controlled Release*, 2018, **275**, 129–141.
135 K. M. Bajjuri, Y. Liu, C. Liu and S. C. Sinha, *ChemMedChem*, 2011, **6**, 54–59.

136 C.-W. Mai, F.-L. F. Chung and C.-O. Leong, *Curr. Drug Targets*, 2017, **18**, 1259–1268.
137 D. Maity, *Beilstein J. Org. Chem.*, 2020, **16**, 2971–2982.
138 W. D. Lubell, *Biomedicines*, 2022, **10**, 2037.
139 J. Chan, S. C. Dodani and C. J. Chang, *Nat. Chem.*, 2012, **4**, 973–984.
140 A. Nadler and C. Schultz, *Angew. Chem., Int. Ed.*, 2013, **52**, 2408–2410.
141 J. R. Lakowicz, *Principles of fluorescence spectroscopy*, Springer, 2006.
142 J. B. Grimm, L. M. Heckman and L. D. Lavis, in *Progress in Molecular Biology and Translational Science*, ed. M. C. Morris, Academic Press, 2013, vol. 113, pp. 1–34.
143 Q. Zheng and L. D. Lavis, *Curr. Opin. Chem. Biol.*, 2017, **39**, 32–38.
144 G. G. Guilbault and D. N. Kramer, *Anal. Chem.*, 1965, **37**, 120–123.
145 B. Rotman, *Proc. Natl. Acad. Sci. U. S. A.*, 1961, **47**, 1981–1991.
146 D. N. Kramer and G. G. Guilbault, *Anal. Chem.*, 1963, **35**, 588–589.
147 B. Rotman, J. A. Zderic and M. Edelstein, *Proc. Natl. Acad. Sci. U. S. A.*, 1963, **50**, 1–6.
148 B. Rotman and B. W. Papermaster, *Proc. Natl. Acad. Sci. U. S. A.*, 1966, **55**, 134–141.
149 F. Coutlee, R. P. Viscidi and R. H. Yolken, *J. Clin. Microbiol.*, 1989, **27**, 1002–1007.
150 S. Xu, Q. Wang, Q. Zhang, L. Zhang, L. Zuo, J.-D. Jiang and H.-Y. Hu, *Chem. Commun.*, 2017, **53**, 11177–11180.
151 K. H. Jones and J. A. Senft, *J. Histochem. Cytochem.*, 1985, **33**, 77–79.
152 Y. Tan, L. Zhang, K. H. Man, R. Peltier, G. Chen, H. Zhang, L. Zhou, F. Wang, D. Ho, S. Q. Yao, Y. Hu and H. Sun, *ACS Appl. Mater. Interfaces*, 2017, **9**, 6796–6803.
153 S. Biswas, B. S. McCullough, E. S. Ma, D. LaJoie, C. W. Russell, D. Garrett Brown, J. L. Round, K. S. Ullman, M. A. Mulvey and A. M. Barrios, *Chem. Commun.*, 2017, **53**, 2233–2236.
154 Z. Qiu, J. Shu and D. Tang, *Anal. Chem.*, 2017, **89**, 5152–5160.
155 S. Lv, Y. Tang, K. Zhang and D. Tang, *Anal. Chem.*, 2018, **90**, 14121–14125.
156 F. Zu, F. Yan, Z. Bai, J. Xu, Y. Wang, Y. Huang and X. Zhou, *Microchim. Acta*, 2017, **184**, 1899–1914.
157 S. Doose, H. Neuweiler and M. Sauer, *ChemPhysChem*, 2009, **10**, 1389–1398.
158 M. Sikorski, E. Krystkowiak and R. P. Steer, *J. Photochem. Photobiol., A*, 1998, **117**, 1–16.
159 C. Geraghty, C. Wynne and R. B. P. Elmes, *Coord. Chem. Rev.*, 2021, **437**, 213713.
160 Z. Lin, M. Li, S. Lv, K. Zhang, M. Lu and D. Tang, *J. Mater. Chem. B*, 2017, **5**, 8506–8513.
161 Z. Yin, L. Zhu, Z. Lv, M. Li and D. Tang, *Talanta*, 2021, **233**, 122563.
162 A. G. Gavriel, M. R. Sambrook, A. T. Russell and W. Hayes, *Polym. Chem.*, 2022, **13**, 3188–3269.
163 A. Dal Corso, S. Arosio, N. Arrighetti, P. Perego, L. Belvisi, L. Pignataro and C. Gennari, *Chem. Commun.*, 2021, **57**, 7778–7781.
164 W. Chyan and R. T. Raines, *ACS Chem. Biol.*, 2018, **13**, 1810–1823.
165 F. W. J. Teale and G. Weber, *Biochem. J.*, 1957, **65**, 476–482.
166 G. Pandit, K. Roy, U. Agarwal and S. Chatterjee, *ACS Omega*, 2018, **3**, 3143–3155.
167 K.-I. Min, G. Yun, Y. Jang, K.-R. Kim, Y. H. Ko, H.-S. Jang, Y.-S. Lee, K. Kim and D.-P. Kim, *Angew. Chem., Int. Ed.*, 2016, **55**, 6925–6928.
168 K. R. Grigoryan and H. A. Shilajyan, *Proceedings of the YSU B: Chemical and Biological Sciences*, 2017, **51**, 3–7.
169 A. B. T. Ghisaidoobe and S. J. Chung, *Int. J. Mol. Sci.*, 2014, **15**, 22518–22538.
170 A. Handelman, N. Kuritz, A. Natan and G. Rosenman, *Langmuir*, 2016, **32**, 2847–2862.
171 P. D. Adams, Y. Chen, K. Ma, M. G. Zagorski, F. D. Sönnichsen, M. L. McLaughlin and M. D. Barkley, *J. Am. Chem. Soc.*, 2002, **124**, 9278–9286.
172 E. Faggi, Y. Pérez, S. V. Luis and I. Alfonso, *Chem. Commun.*, 2016, **52**, 8142–8145.
173 S. Biswas, S. Samui, A. Chakraborty, S. Biswas, D. De, U. Ghosh, A. K. Das and J. Naskar, *Biochem. Biophys. Rep.*, 2017, **11**, 112–118.
174 L. Merkel, M. G. Hoesl, M. Albrecht, A. Schmidt and N. Budisa, *ChemBioChem*, 2010, **11**, 305–314.
175 P. Talukder, S. Chen, B. Roy, P. Yakovchuk, M. M. Spiering, M. P. Alam, M. M. Madathil, C. Bhattacharya, S. J. Benkovic and S. M. Hecht, *Biochemistry*, 2015, **54**, 7457–7469.
176 A. Fernandez, E. J. Thompson, J. W. Pollard, T. Kitamura and M. Vendrell, *Angew. Chem., Int. Ed.*, 2019, **58**, 16894–16898.
177 M. H. Y. Cheng, H. Savoie, F. Bryden and R. W. Boyle, *Photochem. Photobiol. Sci.*, 2017, **16**, 1260–1267.
178 P. N. Joshi and V. Rai, *Chem. Commun.*, 2019, **55**, 1100–1103.
179 C. López-Abarrategui, A. Alba, O. N. Silva, O. Reyes-Acosta, I. M. Vasconcelos, J. T. A. Oliveira, L. Migliolo, M. P. Costa, C. R. Costa, M. R. R. Silva, H. E. Garay, S. C. Dias, O. L. Franco and A. J. Otero-González, *Biochimie*, 2012, **94**, 968–974.
180 L. Mendive-Tapia, C. Zhao, A. R. Akram, S. Preciado, F. Albericio, M. Lee, A. Serrels, N. Kielland, N. D. Read, R. Lavilla and M. Vendrell, *Nat. Commun.*, 2016, **7**, 10940.
181 Y. Zhu, S. Mohapatra and J. C. Weisshaar, *Biophys. J.*, 2019, **116**, 138a.
182 B.-H. Gan, T. N. Siriwardena, S. Javor, T. Darbre and J.-L. Reymond, *ACS Infect. Dis.*, 2019, **5**, 2164–2173.
183 C. Zhao, A. Fernandez, N. Avlonitis, G. Vande Velde, M. Bradley, N. D. Read and M. Vendrell, *ACS Comb. Sci.*, 2016, **18**, 689–696.
184 R. Fischer, T. Waizenegger, K. Köhler and R. Brock, *Biochim. Biophys. Acta, Biomembr.*, 2002, **1564**, 365–374.
185 F. Illien, N. Rodriguez, M. Amoura, A. Joliot, M. Pallerla, S. Cribier, F. Burlina and S. Sagan, *Sci. Rep.*, 2016, **6**, 36938.
186 D. Birch, M. V. Christensen, D. Staerk, H. Franzyk and H. M. Nielsen, *Biochim. Biophys. Acta, Biomembr.*, 2017, **1859**, 2483–2494.

187 M. Sainlos, W. S. Iskenderian and B. Imperiali, *J. Am. Chem. Soc.*, 2009, **131**, 6680–6682.
188 W. Wang, T. Uzawa, N. Tochio, J. Hamatsu, Y. Hirano, S. Tada, H. Saneyoshi, T. Kigawa, N. Hayashi, Y. Ito, M. Taiji, T. Aigaki and Y. Ito, *Chem. Commun.*, 2014, **50**, 2962–2964.
189 W. Wang, L. Zhu, Y. Hirano, M. Kariminavargani, S. Tada, G. Zhang, T. Uzawa, D. Zhang, T. Hirose, M. Taiji and Y. Ito, *Anal. Chem.*, 2016, **88**, 7991–7997.
190 V. Y. Postupalenko, O. M. Zamotaiev, V. V. Shvadchak, A. V. Strizhak, V. G. Pivovarenko, A. S. Klymchenko and Y. Mely, *Bioconjugate Chem.*, 2013, **24**, 1998–2007.
191 H. Chen, J. Scherkenbeck, T. Zdobinsky and H. Antonicek, *Protein Pept. Lett.*, 2010, **17**, 431–436.
192 A. R. Akram, N. Avlonitis, E. Scholefield, M. Vendrell, N. McDonald, T. Aslam, T. H. Craven, C. Gray, D. S. Collie, A. J. Fisher, P. A. Corris, T. Walsh, C. Haslett, M. Bradley and K. Dhaliwal, *Sci. Rep.*, 2019, **9**, 8422.
193 J. Ge, L. Li and S. Q. Yao, *Chem. Commun.*, 2011, **47**, 10939–10941.
194 M. C. Heffern, L. M. Matosziuk and T. J. Meade, *Chem. Rev.*, 2014, **114**, 4496–4539.
195 J.-C. G. Bünzli, *J. Lumin.*, 2016, **170**, 866–878.
196 S. V. Eliseeva and J.-C. G. Bünzli, *Chem. Soc. Rev.*, 2010, **39**, 189–227.
197 Y. Jia, C. M. Quinn, A. I. Gagnon and R. Talanian, *Anal. Biochem.*, 2006, **356**, 273–281.
198 S. H. Hewitt and S. J. Butler, *Chem. Commun.*, 2018, **54**, 6635–6647.
199 E. G. Moore, A. P. S. Samuel and K. N. Raymond, *Acc. Chem. Res.*, 2009, **42**, 542–552.
200 J. C. G. Bünzli, *Coord. Chem. Rev.*, 2015, **293–294**, 19–47.
201 J.-C. G. Bünzli, *Acc. Chem. Res.*, 2006, **39**, 53–61.
202 A. K. R. Junker, M. Tropiano, S. Faulkner and T. J. Sørensen, *Inorg. Chem.*, 2016, **55**, 12299–12308.
203 S. Petoud, S. M. Cohen, J.-C. G. Bünzli and K. N. Raymond, *J. Am. Chem. Soc.*, 2003, **125**, 13324–13325.
204 A. Beeby, I. M. Clarkson, R. S. Dickins, S. Faulkner, D. Parker, L. Royle, A. S. de Sousa, J. A. Gareth Williams and M. Woods, *J. Chem. Soc., Perkin Trans. 2*, 1999, 493–504.
205 I. N. Hegarty, C. S. Hawes and T. Gunnlaugsson, *Org. Chem. Front.*, 2023, **10**, 1915–1926.
206 J. Peuralahti, H. Hakala, V.-M. Mukkala, K. Loman, P. Hurskainen, O. Mulari and J. Hovinen, *Bioconjugate Chem.*, 2002, **13**, 870–875.
207 E. Pazos and M. E. Vázquez, *Biotechnol. J.*, 2014, **9**, 241–252.
208 M. S. Tremblay, Q. Zhu, A. A. Martí, J. Dyer, M. Halim, S. Jockusch, N. J. Turro and D. Sames, *Org. Lett.*, 2006, **8**, 2723–2726.
209 M. S. Tremblay, M. Lee and D. Sames, *Org. Lett.*, 2008, **10**, 5–8.
210 E. Pazos, M. Goličnik, J. L. Mascareñas and M. Eugenio Vázquez, *Chem. Commun.*, 2012, **48**, 9534–9536.
211 H. Jin and J. Varner, *Br. J. Cancer*, 2004, **90**, 561–565.
212 M. Gurrath, G. Müller, H. Kessler, M. Aumailley and R. Timpl, *Eur. J. Biochem.*, 1992, **210**, 911–921.
213 D. Arosio and C. Casagrande, *Adv. Drug Delivery Rev.*, 2016, **97**, 111–143.
214 F. Danhier, A. Le Breton and V. Préat, *Mol. Pharmaceutics*, 2012, **9**, 2961–2973.
215 K. Temming, R. M. Schiffelers, G. Molema and R. J. Kok, *Drug Resistance Updates*, 2005, **8**, 381–402.
216 M. Cieslikiewicz-Bouet, S. V. Eliseeva, V. Aucagne, A. F. Delmas, I. Gillaizeau and S. Petoud, *RSC Adv.*, 2019, **9**, 1747–1751.
217 R. Kumar, W. S. Shin, K. Sunwoo, W. Y. Kim, S. Koo, S. Bhuniya and J. S. Kim, *Chem. Soc. Rev.*, 2015, **44**, 6670–6683.
218 M. H. Lee, J. Y. Kim, J. H. Han, S. Bhuniya, J. L. Sessler, C. Kang and J. S. Kim, *J. Am. Chem. Soc.*, 2012, **134**, 12668–12674.
219 T. Kim, H. M. Jeon, H. T. Le, T. W. Kim, C. Kang and J. S. Kim, *Chem. Commun.*, 2014, **50**, 7690–7693.
220 H.-F. Chau, Y. Wu, W.-Y. Fok, W. Thor, W. C.-S. Cho, P. A. Ma, J. Lin, N.-K. Mak, J.-C. G. Bünzli, L. Jiang, N. J. Long, H. L. Lung and K.-L. Wong, *JACS Au*, 2021, **1**, 1034–1043.
221 H. Y. Shair Kathy, M. Bendt Katharine, H. Edwards Rachel, N. Nielsen Judith, T. Moore Dominic and N. Raab-Traub, *J. Virol.*, 2012, **86**, 5352–5365.
222 J. J. Juarez-Vignon Whaley, M. Afkhami, S. Sampath, A. Amini, D. Bell and V. M. Villaflor, *Curr. Treat. Options Oncol.*, 2023, **24**, 845–866.
223 C.-F. Chan, R. Lan, M.-K. Tsang, D. Zhou, S. Lear, W.-L. Chan, S. L. Cobb, W.-K. Wong, J. Hao, W.-T. Wong and K.-L. Wong, *J. Mater. Chem. B*, 2015, **3**, 2624–2634.
224 W. He, J. Yan, L. Wang, B. Lei, P. Hou, W. Lu and P. X. Ma, *Biomaterials*, 2019, **206**, 13–24.
225 M. Reches and E. Gazit, *Science*, 2003, **300**, 625–627.
226 P. Zhu, X. Yan, Y. Su, Y. Yang and J. Li, *Chem. – Eur. J.*, 2010, **16**, 3176–3183.
227 X. Liu, J. Fei, A. Wang, W. Cui, P. Zhu and J. Li, *Angew. Chem., Int. Ed.*, 2017, **56**, 2660–2663.
228 M. Reches and E. Gazit, *Nat. Nanotechnol.*, 2006, **1**, 195–200.
229 L. Adler-Abramovich, D. Aronov, P. Beker, M. Yevnin, S. Stempler, L. Buzhansky, G. Rosenman and E. Gazit, *Nat. Nanotechnol.*, 2009, **4**, 849–854.
230 Z. A. Arnon, A. Vitalis, A. Levin, T. C. T. Michaels, A. Caflisch, T. P. J. Knowles, L. Adler-Abramovich and E. Gazit, *Nat. Commun.*, 2016, **7**, 13190.
231 Q. Zou, K. Liu, M. Abbas and X. Yan, in *Supramolecular Chemistry of Biomimetic Systems*, ed. J. Li, Springer Singapore, Singapore, 2017, pp. 135–163.
232 K. Tao, P. Makam, R. Aizen and E. Gazit, *Science*, 2017, **358**, eaam9756.
233 R. V. Ulijn and A. M. Smith, *Chem. Soc. Rev.*, 2008, **37**, 664–675.
234 C. A. E. Hauser and S. Zhang, *Nature*, 2010, **468**, 516–517.
235 Z. Fan, L. Sun, Y. Huang, Y. Wang and M. Zhang, *Nat. Nanotechnol.*, 2016, **11**, 388–394.
236 R. M. Wachter, M.-A. Elsliger, K. Kallio, G. T. Hanson and S. J. Remington, *Structure*, 1998, **6**, 1267–1277.

237 D. P. Barondeau, C. J. Kassmann, J. A. Tainer and E. D. Getzoff, *J. Am. Chem. Soc.*, 2002, **124**, 3522–3524.
238 M. L. Contreras, C. Torres, I. Villarroel and R. Rozas, *Struct. Chem.*, 2019, **30**, 369–384.
239 S. Yi, Y. Wang, Y. Huang, L. Xia, L. Sun, S. C. Lenaghan and M. Zhang, *J. Biomed. Nanotechnol.*, 2014, **10**, 1016–1029.
240 B. Gidwani, V. Sahu, S. S. Shukla, R. Pandey, V. Joshi, V. K. Jain and A. Vyas, *J. Drug Delivery Sci. Technol.*, 2021, **61**, 102308.
241 L. Yao, Y. Hu, Z. Liu, X. Ding, J. Tian and J. Xiao, *Mol. Pharmaceutics*, 2019, **16**, 846–855.
242 R. C. Dutta, *Ther. Delivery*, 2011, **2**, 231–234.
243 A. Vats, N. S. Tolley, J. M. Polak and J. E. Gough, *Clin. Otolaryngol. Allied Sci.*, 2003, **28**, 165–172.
244 A. V. Persikov, J. A. M. Ramshaw and B. Brodsky, *J. Biol. Chem.*, 2005, **280**, 19343–19349.
245 F. Cisnetti, C. Gateau, C. Lebrun and P. Delangle, *Chem. – Eur. J.*, 2009, **15**, 7456–7469.
246 J. Liang, X. Susan Sun, Z. Yang and S. Cao, *Sci. Rep.*, 2017, **7**, 37626.
247 A. J. Gordon and M. Phyfferoen, *Rev. Infect. Dis.*, 1983, **5**, S188–S199.
248 İ. Gürsel, F. Korkusuz, F. Türesin, N. Gürdal Alaeddinoğlu and V. Hasırcı, *Biomaterials*, 2000, **22**, 73–80.
249 X. Yan, Y. Cui, Q. He, K. Wang and J. Li, *Chem. Mater.*, 2008, **20**, 1522–1526.
250 X. Wang, W. Zhou, R. Xu, Y. Xu, H. Song, H. Li and J. Wang, *J. Colloid Interface Sci.*, 2023, **645**, 466–471.
251 R. Pugliese, M. Montuori and F. Gelain, *Nanoscale Adv.*, 2022, **4**, 447–456.
252 K. Liu, R. Zhang, Y. Li, T. Jiao, D. Ding and X. Yan, *Adv. Mater. Interfaces*, 2017, **4**, 1600183.